Title
Characterization of Tau and Anticancer Drug Interactions with Microtubules via Cryo-Electron Microscopy Studies

Author
Hejab, Nisreen M A

Publication Date
2016

Peer reviewed|Thesis/dissertation

Characterization of Tau and Anticancer Drug Interactions with Microtubules via Cryo-Electron Microscopy Studies

by

Nisreen M.A. Hejab

A dissertation submitted in partial satisfaction of the

requirements for the degree of

Doctor of Philosophy

in

Comparative Biochemistry

in the

Graduate Division

of the

University of California, Berkeley

Committee in charge:
Professor Kenneth H. Downing, Co-chair
Professor Fenyong Liu, Co-chair
Professor Evange Nogales De La Morena
Professor Mina J. Bissell

Spring 2016

Characterization of Tau and Anticancer Drug Interactions
with Microtubules via Cryo-Electron Microscopy Studies

By

Nisreen M.A. Hejab

Abstract

Characterization of Tau and Anticancer Drug Interactions
With Microtubules via Cryo-Electron Microscopy studies

by

Nisreen M.A. Hejab

Doctor of Philosophy in Comparative Biochemistry

University of California, Berkeley

Professor Kenneth H. Downing, Co-chair

Professor Fenyong Liu, Co-chair

Abstract

Microtubules (MTs) are essential components of the eukaryotic cytoskeleton. They form by the polymerization of tubulin into cylindrical polymers composed of protofilaments. MTs are involved in a diverse array of cellular functions due to their dynamic instability, which is modulated by many factors in vivo and in vitro. Agents that modulate MT dynamics include MT associated proteins (MAPs) and naturally occurring compounds known as MT stabilizing agents (MSAs). A number of MSAs have demonstrated or predicted potential as anticancer agents, but a detailed structural basis for their mechanism of action is still lacking. We have used cryo-electron microscopy (cryo-EM) to study the structural basis of action of zampanolide, a taxane-binding site (TBS) MSA, as well as several proteins known to stabilize MTs, with main focus on tau. We have obtained a high-resolution (4.2 Å) cryo-EM reconstruction of microtubules stabilized by zampanolide and have compared it to Taxol, which binds to the same pocket on β-tubulin. We find that each TBS MSA has distinct structural effects on the microtubule (MT) lattice. Binding of Taxol or zampanolide both induce MT heterogeneity, but each affects the longitudinal interface differently.

Tau is the prominent neuronal MAP and it has been implicated with Alzheimer disease (AD). Tau is known to bind and stabilize MTs in the axons but its binding mode and stabilizing mechanism are not well understood. Our study shows that tau binds exclusively to the external surface of MTs along protofilaments and that it remains in an extended confirmation. In addition, in the presence of kinesin, full length tau (FL-tau) dissociates from MTs allowing kinesin binding. Surprisingly, sub-stoichiometric amounts of tau result in the formation of GDP-tubulin double rings that disappear upon increasing the amounts of tau added to MTs. FL-tau and minimal 2-R or 4-R tau constructs result in the formation of sleeve-like structures around MTs, suggesting that tau binds to tubulin dimers as well as to fully polymerized MTs. Thus, we hypothesize that tau functions by oligomerizing tubulin dimers leading to a compacted MT lattice that could reinforce the interactions across the longitudinal MT interface. Furthermore, we

identified amino acids on the surface of tubulin that could interact with tau. Tau binds to MTs near the C-terminus, and the sequestering of the acidic C-terminus of tubulin could contribute to the stability of MTs in the presence of tau.

To my parents, Mohammed and Mariam, who gave me so much more than life

To my siblings, for always putting a smile on my face

To my best friend and beloved husband, David, who wiped the tears, shared the laughs, picked me up and held my hand throughout the past six years. Without your love, patience and encouragement none of this would have been possible.

Table of Contents
Acknowledgements
List of Abbreviations
List of Figures and Tables

Acknowledgements

First and foremost I would like to thank my advisor Dr. Kenneth Downing for all of his support, advice and encouragement throughout the years. He had an immense role in my personal and professional growth. I also would like to thank Professor Robert Glaeser who always pushed me out of my comfort zone and intellectually challenged me but was also most supportive and helpful. Thanks to Elizabeth Montabana who helped me get the 3100 to work at times, and to Alison Killilea for being the first to teach me how to polymerize MTs. I am also grateful to other people at Donner who helped me with my work including Danielle Jorgens, David Larson, Roseann Csencsits and Puey Ounjai.

I would also like to thank Professor Eva Nogales, who graciously opened her lab to me and provided resources and invaluable advice that made this work possible. I would especially like to thank my collaborator, and dear friend Elizabeth Kellogg, who worked by my side days and nights and supported me beyond the context of this work. I could not have asked for a better mentor and collaborator than Liz. Liz has played a significant role in both the drug and tau work. All the Taxol data provided in this thesis was collected and analyzed by her which allowed for a great comparison with the zampanolide work I conducted. She also helped collect and analyze some of the data sets for tau. I would like to thank the Nogales lab as a whole for all their support, especially Stuart Howes, Rui Zhang who were always happy to help and never complained about my endless emails. Simon Poepsel in the Nogales lab purified all the tau constructs that were used for my studies, and he did it with a smile on his face. Tom Houweling and Patricia Grob had provided technical and microscope support. I would like to acknowledge Dan Van der Mark and Irene Onyeneho for their work on MDM1 and Fam154 A and B, along with Professor Tim Stearns at Stanford University.

I would also like to thank Dr. Fenyong Liu and Dr. Mina Bissell for serving on my dissertation committee and for their support and advice.

Last but certainly not least, I would like to thank my friends for indulging me when I complained and family for their love and support. Special thanks to Julie and Dr. Rick DeNapoli, Marcus and Laurel Larson for their unwavering support.

Abbreviations

2-R	2 repeat
4-R	4 repeat
AD	Alzheimer's disease
CDK5	Cyclin-dependent kinase 5
CDX	Doublecortin
DTT	Dithiothreitol
E. coli	Escherichia coli
EB	End Binding Protein
EDTA	Ethylenediaminetetraacetic acid
EGTA	Ethylene glycol tetraacetic acid
EM	Electron microscopy
FL-tau	Full length tau
FSC	Fourier Shell Correlation
GDP	Guanosine diphosphate
GMPCPP	Guanylyl-(alpha, beta)-methylene-diphosphonate
GTP	Guanosine Triphosphate
GTPγS	GTPγS, guanosine 5'-O-[gamma-thio]triphosphate
HEPES	4-(2-hydroxyethyl)-1-piperazineethanesulfonic acid
IR	Inter-repeat
MAP	Microtubule associated protein
MARKs MAP/MT	Affinity regulating kinase (MARKs)
MBP	Maltose Binding Protein
MSA	Microtubule stabilizing Agents
MT	Microtubules
NFT	Neurofibrillary tangles
NP-40	Nonidet P-40 detergent
PF	Protofilaments
P-gp	P-glycoprotein
PHFs	paired helical filaments
PIPES	Piperazine-N,N′-bis(2-ethanesulfonic acid)
SAP	Stress activated protein kinases
SDS	Sodium Dodecyl Sulfate
SDS-PAGE	SDS-Polyacrylimide Gel Electrophoresis
TMV-MP	Tobacco Mosaic Virus Movement protein
TSB	Taxol-site binders

List of Figures

List of Tables

Chapter One: INTRODUCTION

1.1 Structure of Microtubules and dynamic instability

Microtubules (MTs) are hollow elements in the cytoplasm of all eukaryotic cells. They play a pivotal role in vital cell functions including cell division, morphogenesis, and intracellular transport. Microtubules are highly dynamic polar polymers consisting of αβ-tubulin heterodimers that arrange longitudinally head to tail to form protofilaments (pfs) (Desai & Mitchison 1997, Mitchison & Kirschner 1984). The protofilaments quickly associate laterally into more stable sheets and eventually, the sheets wrap around to form a microtubule with (usually) 13 protofilaments as shown in Figure 1.1 (Akhmanova & Steinmetz 2008). The helical arrangement of the tubulin monomers is due to the staggering of laterally interacting protofilaments. The lateral interactions within a microtubule can be either homotypic, resulting in what is known as a B-lattice microtubule, or heterotypic, resulting in an A-lattice microtubule (Amos and Klug 1974, McIntosh et al. 2009). In the B-lattice microtubule, α-α or β-β tubulin interact with each other, whereas in the less common A-lattice microtubule, β-α or α-β tubulin interact with one another (Amos and Klug 1974). The most abundant type of microtubules found in vivo are 13-pf microtubules with a B-lattice (Tinley et al. 1973). This type of microtubule is pseudo-helical due to the presence of a so-called “seam” where two protofilaments interact with one another in a heterotypic fashion.

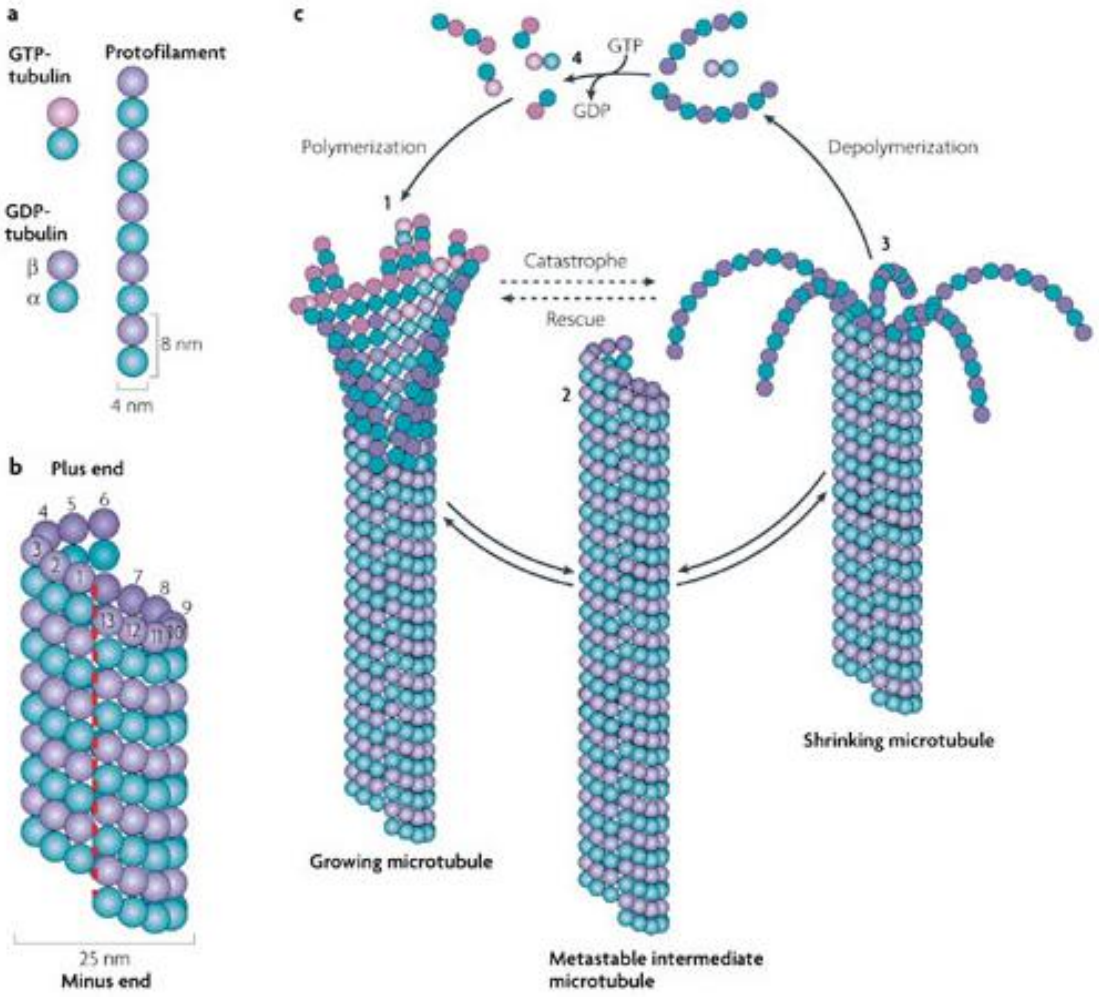

Figure 1.1: **MT structure and dynamic instability**. A) Tubulin dimers consisting of α- and β-tubulin arrange head to tail into a protofilament. B) Protofilaments associate laterally into a MT with a seam which is depicted in a red dash-line. C) Dynamic instability cycle of a MT switching stochastically into growing and shrinking phases. Adapted from Akhmanova & Steinmetz, 2008.

Microtubules grow by the addition of subunits to the ends of protofilaments composing the microtubule wall. Microtubules are polar polymers with distinctive ends, the so called minus end which is capped by α-tubulin and the more dynamic plus end which is capped by β-tubulin (Mitchison 1993, Nogales et al. 1999). Generally, in vivo, the minus-end is anchored to the centriole or microtubule organizing center, whereas the plus-end extends into the cellular space and interacts with cellular elements such as microtubule associated proteins (MAPs) and microtubule binding drugs that regulate the microtubules' dynamics and function (Kreis and Vale 1999, Schiff et al. 1979, Mitchison et al. 1984). If the free tubulin concentration is adequate, a dynamic microtubule can continuously grow from either end. Microtubule polymerization is also GTP-dependent and each α and β tubulin monomer binds to one molecule of GTP (Figure 1.2). The binding of GTP is nonexchangeable in α-tubulin (N-site) whereas it is exchangeable in β-tubulin (E-site). Upon the polymerization of the tubulin dimers, GTP in the E-site of the β-tubulin is hydrolyzed and the GDP in the E-site becomes nonexchangeable. If the rate of polymerization is faster than the rate of GTP hydrolysis, a cap of GTP-bound subunits is

generated at the plus end, although the bulk of β-tubulin in a microtubule will contain GDP. It is thought that the metastable structure of microtubules is stabilized by the so-called GTP cap (Mitchison et al. 1984, Carlier et al. 1984).

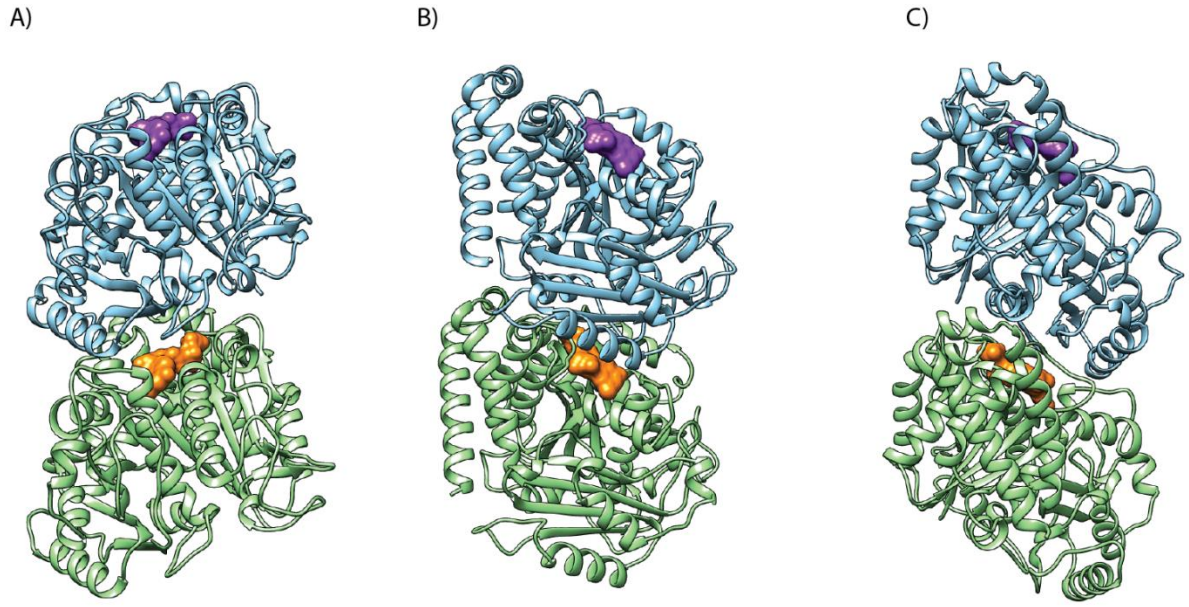

Figure1.2: **Tubulin dimer structure**. A) Inner view of tubulin dimer. B) Side view of tubulin dimer C) outer view of tubulin dimer. α-tubulin is in green and β-tubulin in blue. Nucleotide is colored orange (The N-site) or purple (E-site). Structure of GDP bound tubulin, PDB ID: 3JAS from Zhang et al., 2015.

The α- and β-tubulin monomers are approximately 450 amino acids (aa) long, globular proteins with more than 40% sequence homology (Sander et al. 1991). Each of the monomers consists of 3 globular domains, namely the N-terminal domain (also called GTP-binding domain) and the activation domain which are separated by the central helix H7. The nucleotide binding N-terminal consists of six parallel β-strands alternating with six α-helices (Figure 1.3). The activation domain is formed by three helices and mixed β sheets and is important for lateral and longitudinal interactions between tubulin subunits. The C-terminal mainly consists of two antiparallel helixes (H11 and H12) that cross over the first two domains and it is essential for the regulation of microtubules due to its role in binding microtubules associated proteins (Downing 2000a, Downing 2000b, Nogales et al. 1998). Each tubulin monomer binds one GTP at loops T1-T5 of the GTP-binding domain. Upon protofilament assembly, the GTP bound to β-tubulin is hydrolyzed by the interaction with loop T7 and the glutamic acid (E254) of helix H8 of the activation domain of alpha-tubulin. The GTP of α-tubulin remains unhydrolyzed due to the lack of acidic residues at the end of H8 in β-tubulin (β-tubulin has a lysine instead) (Nogales et al. 1998, Erickson 1998, Mukherjee et al. 2001, Scheffers et al. 2002)

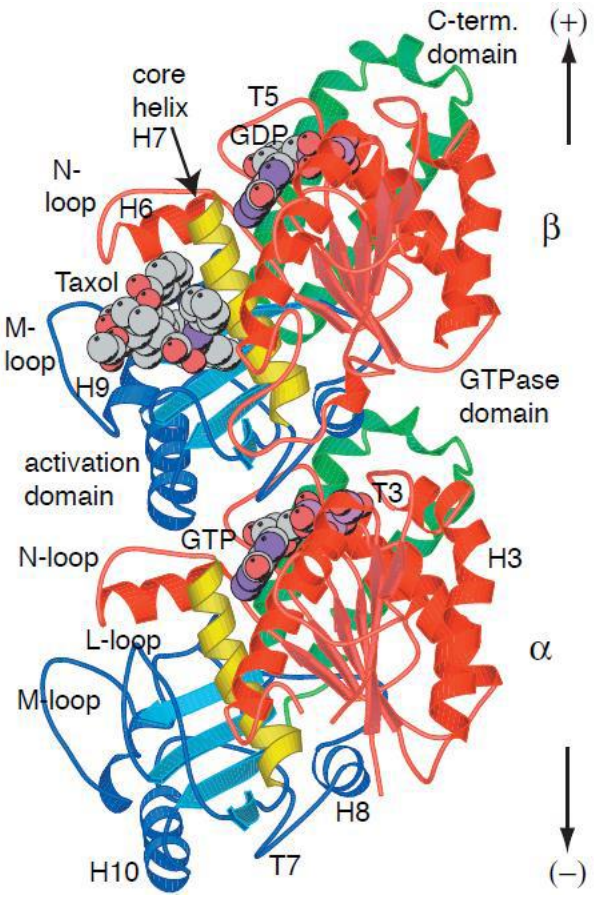

Figure 1.3: **Ribbon diagram of an αβ-tubulin heterodimer of bovine brain tubulin in complex with Taxol** (Nogales *et al.*, 1998; Lowe et al., 2001), with an orientation corresponding to the inside view of a microtubule. The colors depicted in this diagram are as follows: The GTP binding domain is in red, the activation domains in blue. The core helix is yellow and the C-terminal domain on the external surface is green. GTP is sandwiched between the β-tubulin subunit and the α subunit of each heterodimer, being bound to the α-tubulin by loops T1-T6, and also makes contact with loop T7 of β-tubulin. The nucleotide bound to β-tubulin has been hydrolyzed to GDP through contact with helix H8 and loop T7 of the activation domain of another α-tubulin subunit. Taxol sits in the pocket of β-tubulin on the inside face of microtubules. In α-tubulin, this pocket is occupied by the extended L-loop. Adapted from Amos, 2004.

GTP hydrolysis is an important step in the ability of microtubules to oscillate between the growing and shrinking phases, a process known as dynamic instability. If the GDP portion of the microtubule becomes exposed, a "catastrophe" event causes a rapid depolymerization. Dynamic microtubules can depolymerize completely or be rescued and regrown. The stochastic characteristic of the microtubules allows for the independent dynamic behavior of the two ends while searching for stabilizing agents in the cell (Kueh et al. 2009). Microtubule dynamics are also regulated by structural accessory proteins or the post translational modification of tubulin. Furthermore, microtubule dynamics are affected by the free tubulin concentration, which is regulated by the transcription of tubulin and the sequestering of the excess protein (Dumont et al.

2009, Poulain et al. 2010). The dynamic behavior of the tubulin is tightly regulated in the cell and any disruption of the fine-tuned characteristics of the polymer can lead to cell arrest and eventually apoptosis. Such features have led to microtubules being a prominent target for drugs to control maladies, including cancers (Risinger et al. 2009, Hodge et al. 2009).

1.2 Microtubule stabilizing drugs

There is a wide range of natural compounds that target eukaryotic tubulin which are either used by predators as broad-spectrum toxins to inactivate prey or as defenses in more sedentary organisms. Most of these naturally occurring compounds interact with all isotypes of tubulin. A wide range of small molecules, including alkaloids, macrolides and peptides, are known to bind tubulin and enhance or suppress microtubule assembly dynamics by shifting the equilibrium between free dimers and assembled microtubules through various mechanisms. For instance, the presence of Taxol does not alter the hydrolysis of GTP; on the other hand, colchicine increases the hydrolysis of GTP whereas GTP hydrolysis is totally inhibited by vinblastine (Rai & Wolff 1996, Cormier et al. 2010). The structure of such molecules varies greatly (Figure 1.4) and so does their ability to bind and work synergistically or bind competitively to microtubules. Due to their effects on microtubule dynamics, these compounds have been used in a variety of medical applications such as antiparasite agents, herbicides and most importantly, anti-cancer agents (Leroux et al. 2002, Risinger et al. 2009).

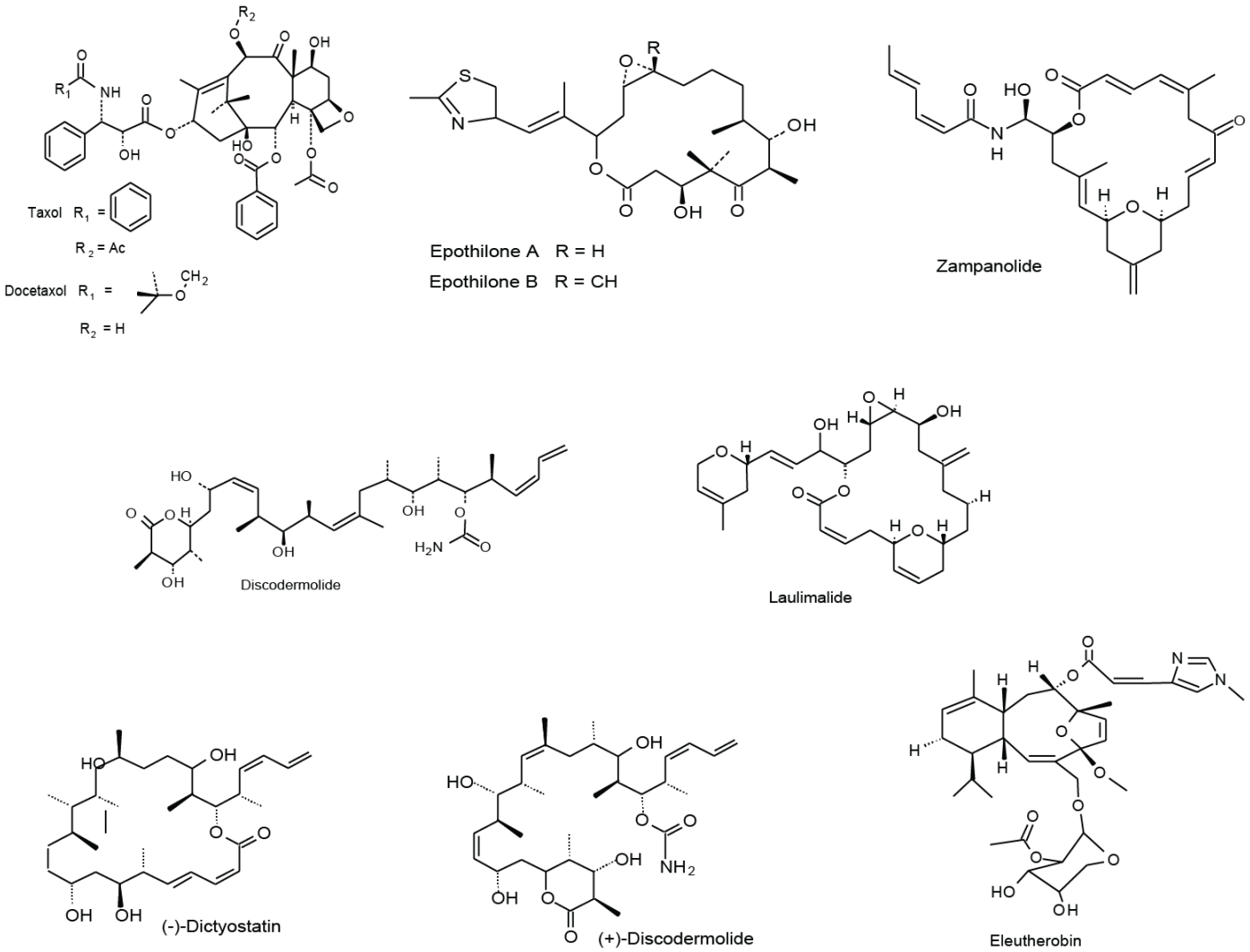

Figure 1.4: Structure of selected MT binding drugs exhibiting the diversity of these compounds

Microtubules are essential in mitosis, during which the chromosomes of a cell are duplicated and separated into two identical sets before cleavage of the mother cell into two daughter cells. Chromosome separation occurs by movement along the microtubules of the spindle. Their importance in mitosis and cell division makes microtubules an important target for anticancer drugs (Jordan & Wilson 1998). Most microtubule-targeted compounds have been discovered as inhibitors of mitosis in large-scale screens of natural products. Among the earliest developed were the vinca alkaloids, which were isolated more than 50 years ago from periwinkle leaves (Jordan & Wilson 2004). Microtubule binding drugs generally bind to one of three main classes of sites on tubulin, the paclitaxel site (taxane site), the vinca domain and the colchicine domain. MT destabilizing drugs bind to tubulin in the vinca or colchicine domain in β-tubulin (Pryor et al. 2002, Huzil et al. 1998). Other binding sites include a proposed imidazole site in β-tubulin and a dinitroaniline site in α-tubulin. MT stabilizing drugs, with the exception of laulimalide and peloruside, bind to the taxane site (Figure 1.5) (Downing 2000). MT binding drugs lead to apoptosis via the suppression of spindle-microtubule dynamics, which leads to blocking of mitosis at the metaphase–anaphase transition (Jordan & Wilson, 2004).

MT binding drugs can be classified into MT stabilizing agents (MSA) which promote MT polymerization and stabilization, and MT destabilizing agents (MDA) which inhibit MT polymerization at high concentrations. MSAs include paclitaxel (Taxol), docetaxel (Taxotere), the epothilones, discodermolide, the eleutherobins, sarcodictyins, laulimalide, rhazinalam, and certain steroids and polyisoprenyl benzophenones (Jordan et al. 2002, Jimenez-Barbero et al. 2002). MDAs include vinca alkaloids (vinblastine, vincristine, vinorelbine, vindesine and vinflunine), cryptophycins, halichondrins, estramustine, colchicine and combretastatins (Boder at al. 1983; Jordan 2002).

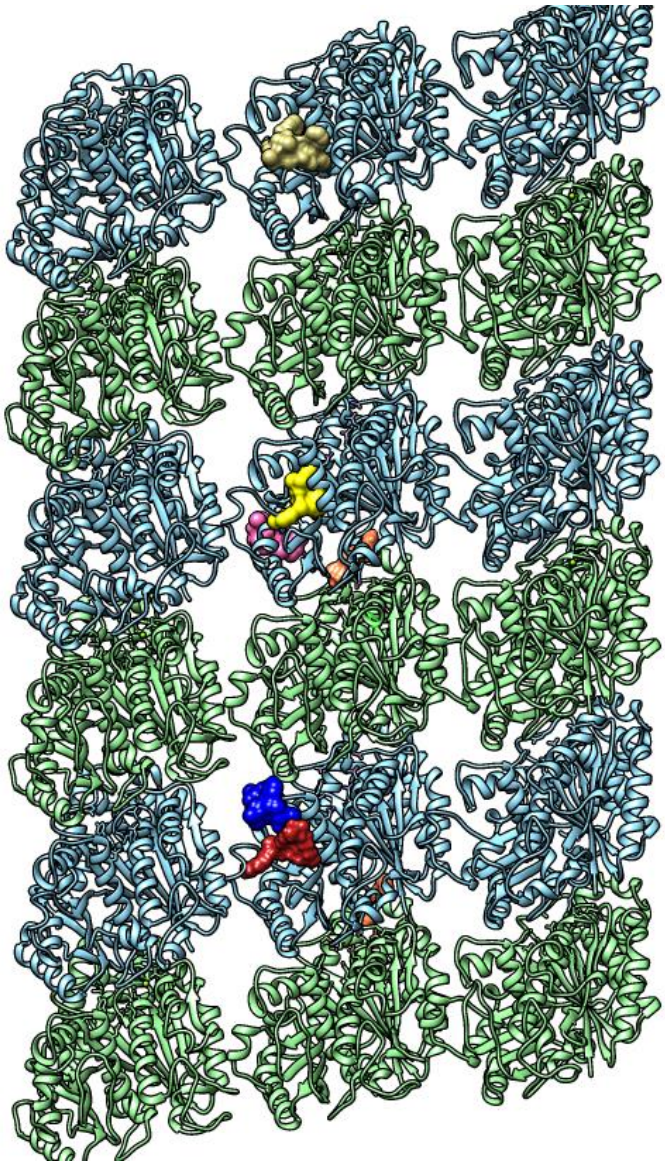

Figure 1.5: Binding location of MT binding drugs as determined by electron and X-ray crystallography. α-tubulin is green, β-tubulin is in blue, epothilione is in yellow (PDB ID 404I), zampanolide is in red (PDB ID 4I4T), vinblastine is in blue (PDB ID 4EB6), peluroside is in pink (PDB ID 404I) colchicine binding pocket is in coral (PDB 5C84), Taxol is in khaki (PDB ID 1JFF)

Microtubule binding drugs affect the MT dynamics in various ways. Some of the drugs bind to free tubulin dimers whereas others bind to tubulin that has been incorporated into the MT lattice. The latter class of drugs is more effective at modulating MT dynamics. Other factors such as binding location of the drug (Figure 1.5), and the type of bond that forms between the drug and tubulin affect its potency as tumor suppressor agent (Kavallaris 2010). Despite the wide usage of some MT binding drugs, such as Taxol, for cancer therapy, the detailed structural basis for their mechanism of action is still lacking. In Chapter 2 I will discuss distinct effects of Taxol, zampanolide and peloruside on the microtubule lattice and microtubule stabilization.

1.3 Microtubule Associated Proteins (MAPs)

In eukaryotic cells, microtubules are able to interact with numerous types of proteins, estimated to be over 400 (Sakamoto et al. 2008). MAPs include motor proteins such as kinesins and dyneins, plus-end tracking proteins such as EB3, centrosome-associated proteins, enzymatically active and structural MAPs (Dehmelt et al. 2005). Microtubule motors, such as kinesin and dynein play essential roles in cellular transport and force generation in eukaryotic cells. Kinesin is generally responsible for transporting cargo towards the MT plus-end whereas dynein moves towards the MT minus end (Hirokawa 1998). ATP hydrolysis is required by motor proteins for their function.

The "classical" MAPs usually bind along the MT lattice, and they stabilize MTs (Bonnet et al. 2001). This class of MAPs was the first to be identified and has been extensively studied. It includes the neuronal MAP1, MAP2 and tau in addition to MAP4 (Keats et al. 1975, Murphy et al. 1975, Sloboda et al. 1976). Other MAPs such as katanin destabilize MTs, which enables the rearrangement of the cytoskeleton as needed during development (Díaz-Valencia 2011). Structural MAPs tend to consist of repeat domains which enable these proteins to interact with more than one tubulin dimer at once leading to their ability to control the assembly and dynamics of microtubules (Amos et al. 2005). The binding of the structural MAPs usually occurs through electrostatic interaction with the acidic C-terminal of tubulin (Serrano et al. 1984). The binding to microtubules is commonly controlled by phosphatases and kinases (Cassimeris et al. 2001). The phosphorylation of these MAPs weakens the electrostatic interaction between the microtubule and the MAP causing the dissociation of the MAP from the microtubule lattice (Horwitz et al. 1997, Chang et al. 2001). In cells undergoing mitosis, structural MAPs become phosphorylated, allowing tubulin assembly and disassembly to be controlled by proteins that bind to the ends of the microtubules (Amos et al. 2005). The phosphorylation of MAPs is accomplished by a large number of kinases including include MAP kinase, casein kinase II, Ca^{2+} calmodulin-dependent protein kinase II, the stress activated protein kinases (SAP), MAP/MT affinity regulating kinase (MARKs), cyclin-dependent kinase 5 (cdk5) (Cassimeris & Spittle 2001).

Among the well-studied mammalian MAPs are the neuronal tau and MAP2, and the non-neuronal MAP4. Homologous proteins have been found in *Xenopus* species and invertebrates (Goedert 1996, Heidary 2001). These MAPs are all predicted to be intrinsically unstructured proteins, lacking any secondary structure elements. Tau and MAP2 contain a microtubule binding domain which consists of three or four 31-residue repeats that are preceded by a projection domain near the N-terminal. Once the MAP is bound to the microtubule, the projection domains that extend from the outer surface of the microtubule seem to repel neighboring microtubules (Cassimeris et al. 2001, Amos et al. 2005). The binding of tau and

MAP2 have been shown to increase the stability of microtubules by reducing the catastrophe events and increasing the rescues (Drechsel et al. 1992). However, the binding location of tau on MTs has been controversial. Tau is the prominent neuronal MAP and it has been implicated with Alzheimer disease (AD). AD is the most common form of dementia and it affects 44 million people worldwide (Alzheimer's Disease International, http://www.alz.org/). The hallmark of AD is the presence of paired helical filaments (PHFs) in brain tissues (Goedert et al. 1988, Kondo et al. 1988). Tau is normally associated with MTs in the axons, but in AD patient brains, tau is hyperphosporylated (Goedert et al. 1992). The phosphorylation of tau leads to its dissociation from MTs, and hyperphosphorylated tau forms PHFs that assemble into neurofibrillary tangles (NFT) which are found in the plaques AD patients (Lee et al. 1991). The phosphorylation of tau in AD patients is not a result of a mutation in tau but it is due to the downregulation of phosphatases and upregulation of kinases that are specific to tau. In some cases such as in frontotemporal dementia, AD is caused by mutations in the microtubule binding domain of tau (Hutton et al. 1998). Chapter 3 of this dissertation describes our work on tau in depth.

Chapter Two: Insights into the distinct mechanisms of action of taxane microtubule stabilizers from Cryo-EM structures

Introduction

Microtubules are crucial components of the cytoskeleton and play a central role in cell-division. Essential to their function is the property of dynamic instability, the stochastic switching between growing and shrinking linked to GTP binding and hydrolysis. Microtubule dynamics are tightly regulated in vivo by a number of microtubule-associated proteins (MAPs). Widely successful chemotherapeutics, such as Taxol, bind to and stabilize MTs, thus inhibiting dynamic instability and preventing cancer cells from dividing (Schiff et al. 1979, Manfredi & Horwitz 1984). Since its discovery (Wani et al. 1971) Taxol has been the subject of many studies aimed at identifying its mechanism of action (Ojima et al. 2014).

Numerous cancer research efforts have been directed towards identifying other natural small-molecules that are able to stabilize MTs or towards synthesizing Taxol-like analogs. As a result, a growing number of taxane and non-taxane microtubule-stabilizing agents (MSAs) have been identified. Today there is a large number of structurally diverse MSAs, including epothilone (Gerth, Bedorf et al. 1996), zampanolide (Tanaka 1996), peloruside (West, Northcote et al. 2000), discodermolide (ter Haar, Kowalski et al. 1996), and laulimalide (Mooberry, Tien et al. 1999) among others. In some cases their binding site on tubulin has been described in atomic detail (Prota et al. 2013; Prota et al. 2014a; Prota et al. 2014b). Many of these agents (such as epothilone and zampanolide) target the Taxol-binding pocket and are generally known as Taxol-site binders (TSBs).

Taxol is a widely used chemotherapeutic agent that has been effective in the treatment of lung, breast and ovarian cancers. Despite its efficacy, Taxol has low solubility in water and it is susceptible to the P-glycoprotein (P-gp) drug efflux pumps which become overexpressed with elongated Taxol usage (Dumontet & Jordan 2010). As a result, drugs that are not affected by the P-gp drug efflux pumps are of particular interest for chemotherapy. In recent years, MSAs that bind to tubulin covalently have been shown to be less susceptible to the P-gp-mediated multidrug resistance (Buey et al., 2007). Zampanolide, a recently discovered MSA (Tanaka & Higa 1996; Field at al. 2009) has been shown to bind covalently to β-tubulin (Field et al. 2012). Zampanolide is a TSB, and while Taxol's effects on MTs have been studied extensively, little is known on how zampanolide binds to and affects MTs. Furthermore, we sought to answer an open question regarding TSBs: whether different drugs within the same class affect the MT lattice differently. TSBs are diverse in their structures, yet they all have the same damping effects on MT dynamic instability.

Taxol binds to a pocket in β-tubulin (Nogales et al. 1998) facing the lumen of a MT, near the lateral interface between protofilaments (Nogales et al. 1998, Nogales et al. 1999, Alushin et al. 2014) (Figure 2.1). It has been reported that the addition of Taxol to dynamic MTs alters their protofilament (PF) distribution (Arnal & Wade 1995, Diaz et al. 1998). In the absence of drugs, dynamic MTs form mostly 13-PF and 14-PF MTs (Wade et al. 1990, Chretien et al. 1992); upon the addition of Taxol, 14-PF MTs become the most dominant species. This observation suggests that the addition of Taxol alters the lateral interface in a MT lattice. Furthermore, Taxol has been shown to straighten individual protofilaments (Elie-Caille et al. 2007). High-resolution cryo-EM studies comparing MTs in different nucleotide states have indicated that GTP hydrolysis leads to a compaction at the longitudinal interdimer interface, adjacent to the nucleotide in β-tubulin

(Alushin et al. 2014, Zhang et al. 2015). Taxol seems to reverse the effect of GTP hydrolysis, giving rise to a lattice expansion (Arnal & Wade 1995, Alushin, Lander et al. 2014). Because the Taxol reconstruction in the workdone by Alushin and Lander et al. was of lower resolution (5.5 Å) than the drug-free states, it was not possible to describe the details of this Taxol-induced lattice expansion. Thus, the allosteric mechanism that links the Taxol-binding pocket to the longitudinal interfaces is still unknown. Little is known on how zampanolide compares to Taxol in the context of a MT lattice and whether the two TSBs share a common mechanism to induce MT stability. Because MSAs are classified based on their binding location, we wanted to compare the effects of two TSBs on the MT lattice.

Crystallographic studies of zampanolide and Taxol focused on the contribution of these MSAs to the stabilization of the M-loop in β-tubulin. Currently, MSAs are proposed to stabilize MTs by facilitating the lateral contacts between protofilaments (Prota at al. 2013; Prota et al. 2014a; Prota et al. 2014b). Due to the nature of crystallographic studies, it is not feasible to address the effects of MSAs in the context of a polymerized MT. The currently available crystallographic studies show very little change outside the drug-binding pockets (Prota et al. 2013, Prota et al. 2014a, Prota et al. 2014b). This could be a limitation of using crystallography to study these subtle effects, or it could be because MSAs do not induce large changes in tubulin conformation upon binding. In this chapter, we sought to study the effects of zampanolide on the MT lattice using cryo-EM and compare them to the effects of Taxol binding. The findings reported in this chapter on Taxol-MT binding are the work of Dr. Elizabeth Kellogg (manuscript in preparation) and her results will be used for comparison with zampanolide.

In spite of the progress over the years, a complete understanding of the stabilizing mechanism of MSAs remains elusive. In addition to gaining insights into MT dynamic instability, understanding how MSAs stabilize MTs is essential for improving MSA design for cancer therapy. Collectively, we found that zampanolide and Taxol have very different effects on MT lattice structure, suggesting that they involve distinct stabilizing mechanisms. In addition, we found that Taxol- and zampanolide-binding results in a similar degree of structural heterogeneity in the MT walls. We find that the differences between the reconstructions at the level of the tubulin-dimer are minimal, in agreement with the x-ray crystallography studies, or cannot be resolved within this resolution regime.

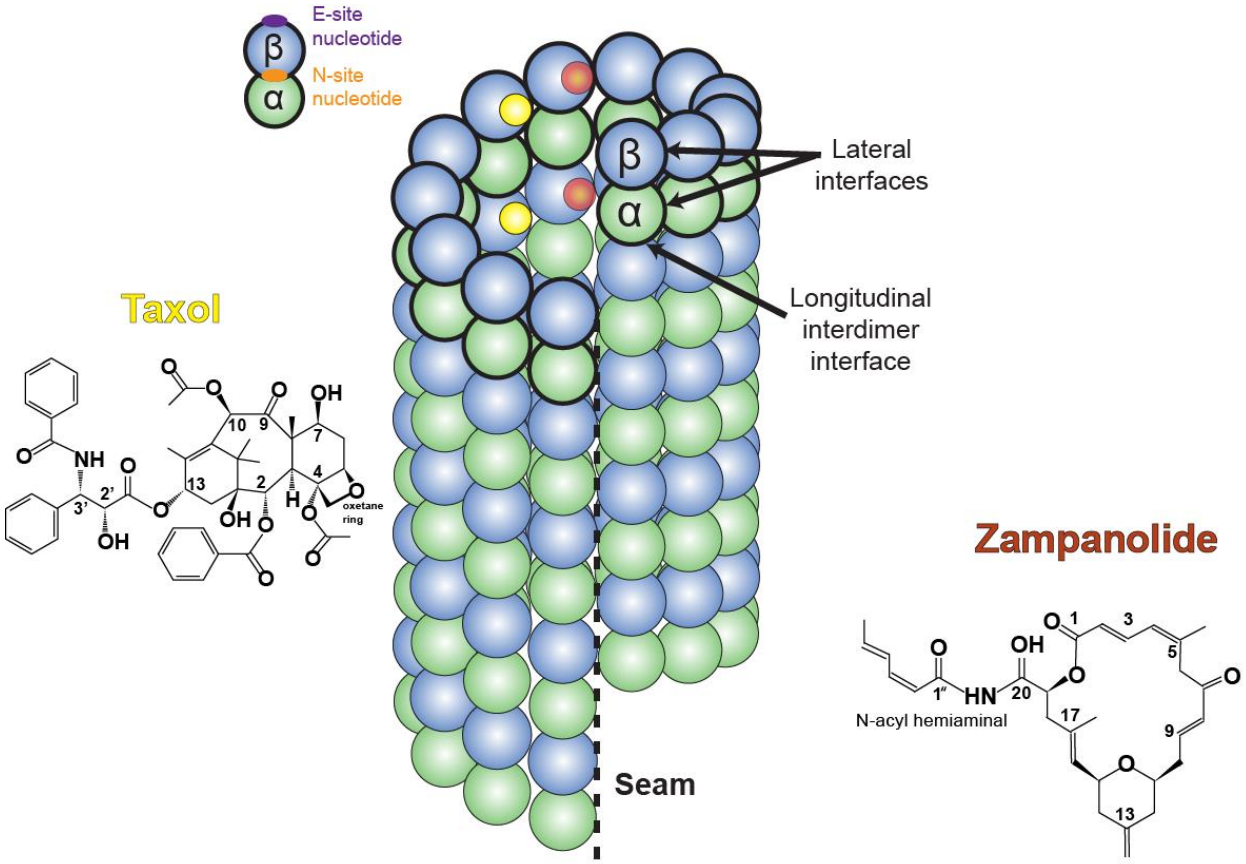

Figure 2.1: Schematic of a microtubule and binding sites for TSB MSAs. Taxol and zampanolide bind to the same lumenal binding pocket

Methods

Microtubule-assembly and vitrification

Lyophilized porcine tubulin (Cytoskeleton Cat # T240) was resuspended to 10mg/ml in EM buffer (80mM PIPES pH 6.8, 1mM EGTA, 1mM $MgCl_2$) supplemented with 10% glycerol and 1 mM GTP. Zampanolide was a gift from Dr. Fernando Diaz, Centro de Investigaciones Biológicas. Due to limited amounts of zampanolide, tubulin aliquots were diluted 4-fold into cold EM buffer supplemented with 10% glycerol (to mimic the buffer used to store tubulin at -80° C), incubated on ice for 15 min, polymerized at 37° C for 15 minutes, and then spun at 17,000 g for 20 minutes using a tabletop centrifuge. The dynamic microtubule pellet was resuspended in 20 µl warm EM buffer containing 1mM GTP and was quickly diluted approximately 6-fold (to a final concentration of 0.5 mg/mL) into warm EM buffer containing 50 µM -100 µM zampanolide. MT absorbance was measured at 280 via a NanoDrop to estimate tubulin concentration.

Kinesin was prepared as described previously (Alushin et al. 2014) and stored in aliquots of 15 µl at -80° C. When ready to be used, aliquots are desalted into EM buffer and kept in 10 µl aliquots on ice until vitrification. A Mark V Vitrobot was used to perform sample vitrification at room temperature (25° C, ambient humidity) and a blot force setting of 10. 2 µl of MTs were

incubated on holey carbon 1.2/1.3 C-flat grids (Protochips) for 30 seconds, then washed twice with 4 µl kinesin, waiting 30 seconds between washes (total incubation time: 2 minutes).

Imaging and post-processing

Data collection proceeded as previously described (Zhang et al. 2015). Images were collected in counting mode on a K2 Summit detector (Gatan), with a total dose of 27.5 e-/A^2. Each exposure was 6 seconds long and comprised a set of 20 frames of 300 ms exposure for each. A 300 kV Titan scope (FEI) was operated at 27,500X magnification with a nominal pixel size of 1.32 Å. Prior to sample insertion, the gun-tilt and coma- alignments were carefully performed. Images were drift-corrected using UCSF driftcorr software (Bai et al. 2013), and particles (MT segments along the length of a MT) were boxed out using overlapping boxes, each box separated by 80 Å along the filament with a box size of 512 pixels (~676 $Å^2$). We used CTFFIND4 (Rohou & Grigorieff 2015) to estimate CTFs for the drift-corrected images. We then estimated global alignment parameters using a multi-reference alignment script (using EMAN2 libraries (Tang et al. 2007), against low-pass filtered (~20 Å) references, comprising 12 -15 protofilaments MT models. The resulting global alignment parameters were used as inputs for refinement in FREALIGN (Lyumkis, Brilot et al. 2013) to obtain 4.2 Å reconstructions. Pseudo-helical symmetry was imposed as previously described (Sindelar and Downing, 2007; Alushin et al. 2014) to generate a 'good' protofilament that was then used to create a full MT model for further refinement. The refinement was carried out for 3 iterations or until reconstruction resolution converged.

In order to characterize the structural heterogeneity in each dataset, we employed RELION 3D classification. We used refined FREALIGN translations and orientations as initial translations/orientations, along with unmasked particles corresponding to a box-size of 400 pixels. C1 reconstructions (asymmetric reconstruction obtained using FREALIGN parameters) were estimated to be at 6-7 Å resolution. Particle-polishing and local refinement improved the resolution to 4-5 Å (Scheres 2014). These refined translations and orientations were then subjected to RELION 3D sorting using fixed alignment parameters for all datasets.

Model-building

Maps were sharpened by using a negative B-factor of 100-150 $Å^{-1}$ and filtered to the resolution estimated using gold-standard FSC. We further filtered the zampanolide map and Taxol map (Elizabeth Kellogg, manuscript in preparation) according to local resolution estimates using bsoft (Heymann et al. 2008). We used as starting atomic model that of the dynamic, GDP-bound state without drug from previous work (Zhang et al. 2015). Ligand conformations were copied from high-resolution crystal structures and were kept fixed throughout refinement, but ligand rigid-body degrees of freedom (translations/rotations) were optimized. GTP and GDP were obtained from 4I4T (Prota et al. 2013) and Taxol from 1JFF (Lowe et al. 2001). A 3x3 dimer section of the MT-lattice was modeled using Rosetta-refinement (DiMaio et al. 2015) as described previously (Alushin et al. 2014). Helical parameters were derived from processing the micrographs and used in docking atomic models into the 3x3 lattice and were subsequently kept fixed throughout atomic refinement. Atomic refinement against the full maps was carried out, producing >1000 models for each map. The lowest 1% of models by total score were selected, and a consensus model was created by averaging backbone coordinates and selecting the most

common rotamer. This representative model was then refined against the map using refmac to produce a final model with optimal geometry and fit to the map.

Refmac refinement was performed, according to the recommended procedure, on a single tubulin-dimer as a final optimization step. ProSMART was used to generate secondary structure and reference-based restraints, using 4I4T as a reference model. LIBG was used to generate ligand restraints, using GTP, GDP and zampanolide coordinates obtained from 4I4T. For zampanolide, one additional covalent bonding restraint was added to maintain appropriate distance between H230 of β-tubulin and the C-9 atom of zampanolide. The final models typically deviated from the initial, starting model by less than 0.5 Å rmsd.

Results

Zampanolide and Taxol have different effects on MT lattice structure

MTs have a high degree of helical symmetry (Figure 2.1) that can be estimated even at sub-nanometer resolution. Because of the symmetry, two tubulin dimers in adjacent protofilaments can be related using three parameters, collectively referred to as the 'lattice parameters': the rise (translation along the helical axis, parallel to the seam), twist (rotation around the helical axis), and the 'supertwist' which describes the position of the seam (0 supertwist means the seam is at the same position throughout the MT). The axial repeat, related to the helical rise, describes the distance between tubulin dimers within a straight protofilament. The axial repeat has been used as a basis for comparing drug-free MT lattice either bound to GMPCPP (corresponding to a GTP-like state), GDP or GTPγS (Zhang et al. 2015). MTs bound to GMPCPP were shown to have an 'expanded lattice' with a 83.1 Å axial repeat whereas the dynamic, GDP-bound MT has a 'compacted lattice' with an axial repeat of 81.6 Å (Zhang et al. 2015). When zampanolide is added to pre-formed MTs, zampanolide-MTs have an axial repeat of 80.8 Å (Table 2.1 A, 2.1 B), distinct from the lattice parameters of the drug-free MT lattice (81.6 Å). Furthermore, the lattice parameters for zampanolide-MTs were distinct of Taxol-MTs that were prepared under similar conditions (81.8Å) (Elizabeth Kellogg, manuscript in preparation). Furthermore, zampanolide-MTs have a supertwist of approximately -0.1° for all collected datasets (Table 2.1 A and B), opposite in direction compared to Taxol-MTs (Elizabeth Kellogg, manuscript in preparation) but similar to that observed in EB3-MTs (Zhang et al. 2015), indicating that the structural effect of zampanolide-binding on the MT lattice is distinct from that of Taxol. When added to unassembled tubulin, Taxol results in a lattice expansion, with an axial repeat of 82.3 Å, consistent with a model in which Taxol inhibits the structural transitions known to occur upon GTP-hydrolysis (Elizabeth Kellogg, manuscript in preparation). Though the measured axial repeat is smaller than previously reported (Alushin, Lander et al. 2014), it is consistently observed to be expanded with respect to the drug-free, dynamic, GDP-MT reconstruction across independent datasets (Table 2.1), indicating that the structural changes, while subtle, are robustly observed (Elizabeth Kellogg, manuscript in preparation).

Previous studies reported that some drugs, such as Taxol, produce different axial repeats when added to unassembled tubulin or pre-formed MTs (Arnal & Wade 1995), suggesting that the structural effects of the drug may be different depending on when it is added: before tubulin incorporation into the lattice, and thus before GTP hydrolysis, or after MT assembly, and thus into a pre-existing GDP-bound state. While these results were confirmed for Taxol-stabilized MTs (Elizabeth Kellogg, manuscript in preparation), we focused on studying the structural

effects of zampanolide addition to preformed MTs due to limited amount of drug. In this study we found that MT polymerization in the presence of zampanolide induces the formation of open-sheet tubulin structures. Such polymers are also observed in the presence of Taxol, but are not as abundant (Figure 2.2). Furthermore, in the presence of zampanolide, 13-PF MTs are the most dominant MTs, whereas Taxol induces the formation of 14-PF MTs, indicating that while both TBSs affect lateral interactions, they have different effects.

Table 2.1A): Lattice parameters for the reconstructions of 13-pf MTs. The values show that zampanolide and Taxol have different effects on the MT structure. Taxol data measured from maps provided by Elizabeth Kellogg.

Drug/nucleotide	when added (pre- or post-lattice formation)	Dimer Rise (Å)	Dimer Twist (°)	Axial Rise (Å)	Axial Twist (°)
Taxol	Post	9.47	-27.7	81.8	0.08
	Post	9.48	-27.7	81.9	0.02
	Pre	9.52	-27.7	82.3	0.10
	Pre	9.52	-27.7	82.3	0.09
Zampanolide	Post	9.40	-27.7	80.8	-0.12
	Post	9.40	-27.7	80.8	-0.09
	Post	9.38	-27.7	80.8	-0.09
GDP-MT (drug-free)	N/A	9.45	-27.7	81.7	0.01
GMPCPP-MT	N/A	9.62	-27.7	83.2	0.20

Table 2.1B): Lattice parameters for the reconstructions of 14-pf MTs. The values show that zampanolide and Taxol have different effects on the MT structure. Taxol data measured from maps provided by Elizabeth Kellogg.

Drug	when added (pre- or post-lattice formation)	Dimer Rise (Å)	Dimer Twist (°)	Axial Rise (Å)	Axial Twist (°)
Taxol	Post	8.79	-25.76	81.9	-0.42
	Post	8.8	-25.80	81.9	-0.40
	Pre	8.7	-25.80	81.9	-0.40
	Pre	8.77	-25.76	81.9	-0.44
Zampanolide	Post	8.6	-25.77	80.7	-0.58
	Post	8.6	-25.77	80.8	-0.59
	Post	8.6	-25.77	80.8	-0.57
GDP-MT (drug-free)	N/A	8.76	-25.76	81.5	-0.46

GMPCPP-MT	N/A	8.92	-25.8	83.1	-0.34

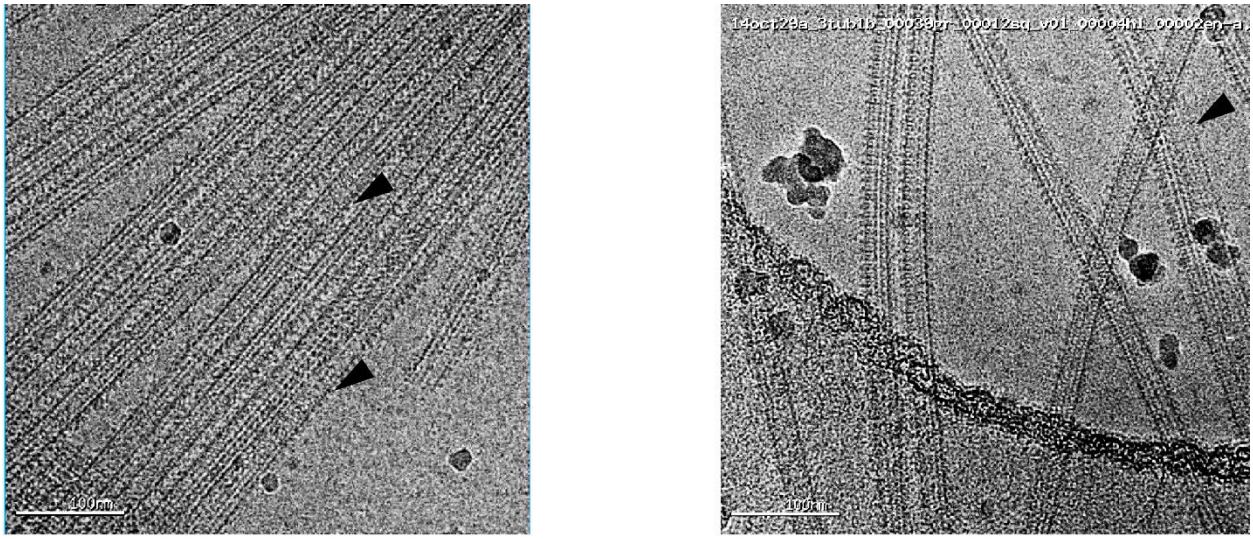

Figure 2.2: Cryo-EM images of MTs bound to zampanolide or Taxol. Zampanolide (left) or Taxol (right) were added during MT polymerization. Open sheets are observed in all cases (indicated by arrows). These open structures are more abundant in the presence of zampanolide. Taxol image provided by Elizabeth Kellogg

Reconstruction features and kinesin binding

Several batches of samples were prepared under identical conditions, and independent data sets were collected and processed as shown in Table 2.1A. To obtain a high, near-atomic resolution cryo-EM reconstruction of zampanolide-MT structure (4.2 Å) (Figure 2.3), we combined all independent data sets that were prepared and collected under identical conditions. β-strand separation, helical pitch, and some sidechain densities are visible throughout the majority of the reconstructions (Figure 2.4), as expected for the reported resolution range. The density for the zampanolide ligand is sufficiently resolved to conclude that its binding mode is in agreement with what was visualized in previous X-ray crystallographic studies in the contexts of tubulin dimers outside of a polymerized MT context (Prota et al. 2013) (Figure 2.3).

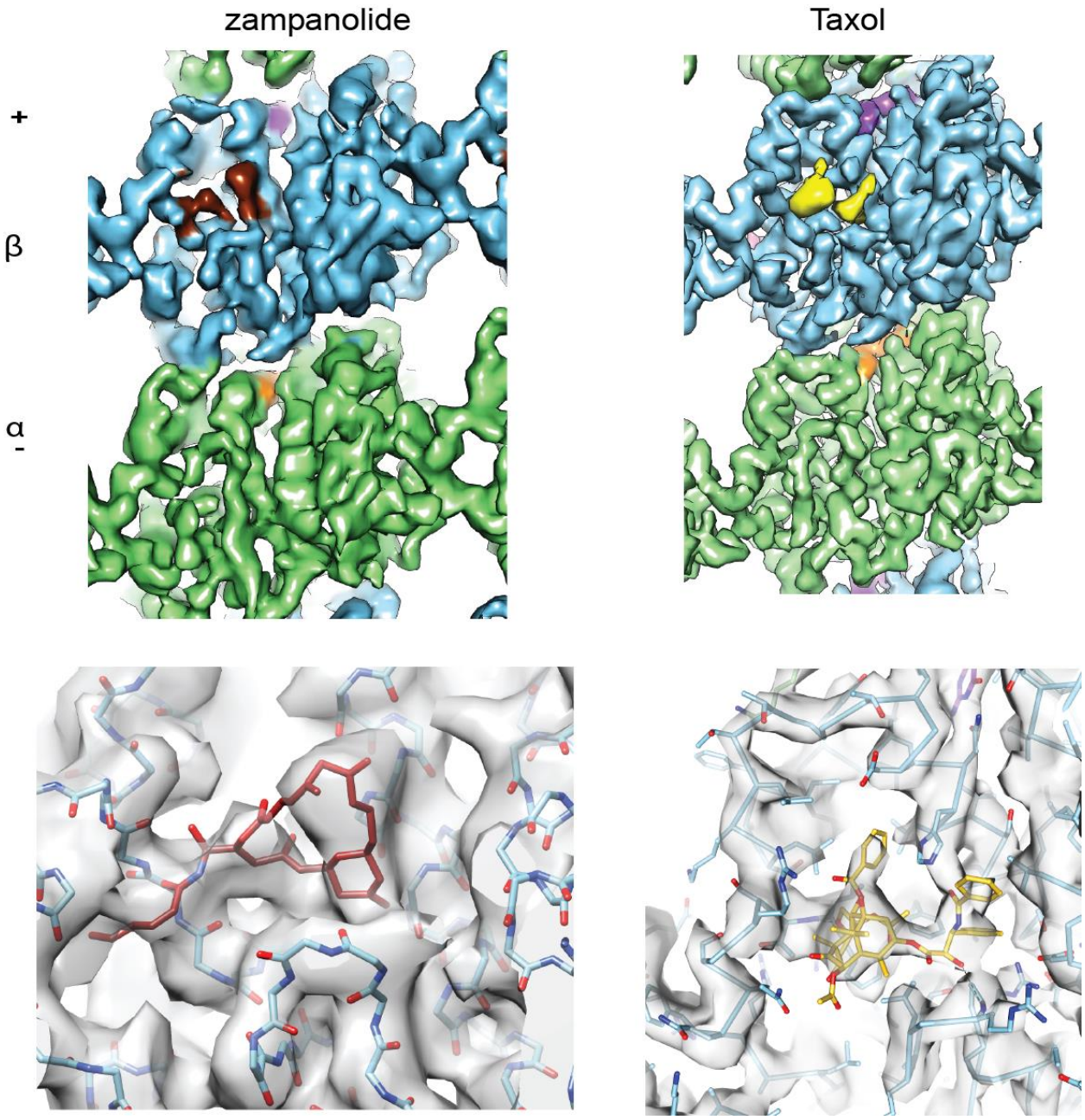

Figure 2.3: Cryo-EM reconstructions and TSBs binding pockets. A) Structures for MTs bound to zampanolide (4.3 Å, left) and of Taxol (3.9 Å, right Elizabeth Kellogg, manuscript in preparation. Zampanolide- and Taxol-bound MTs are seen from the lumen

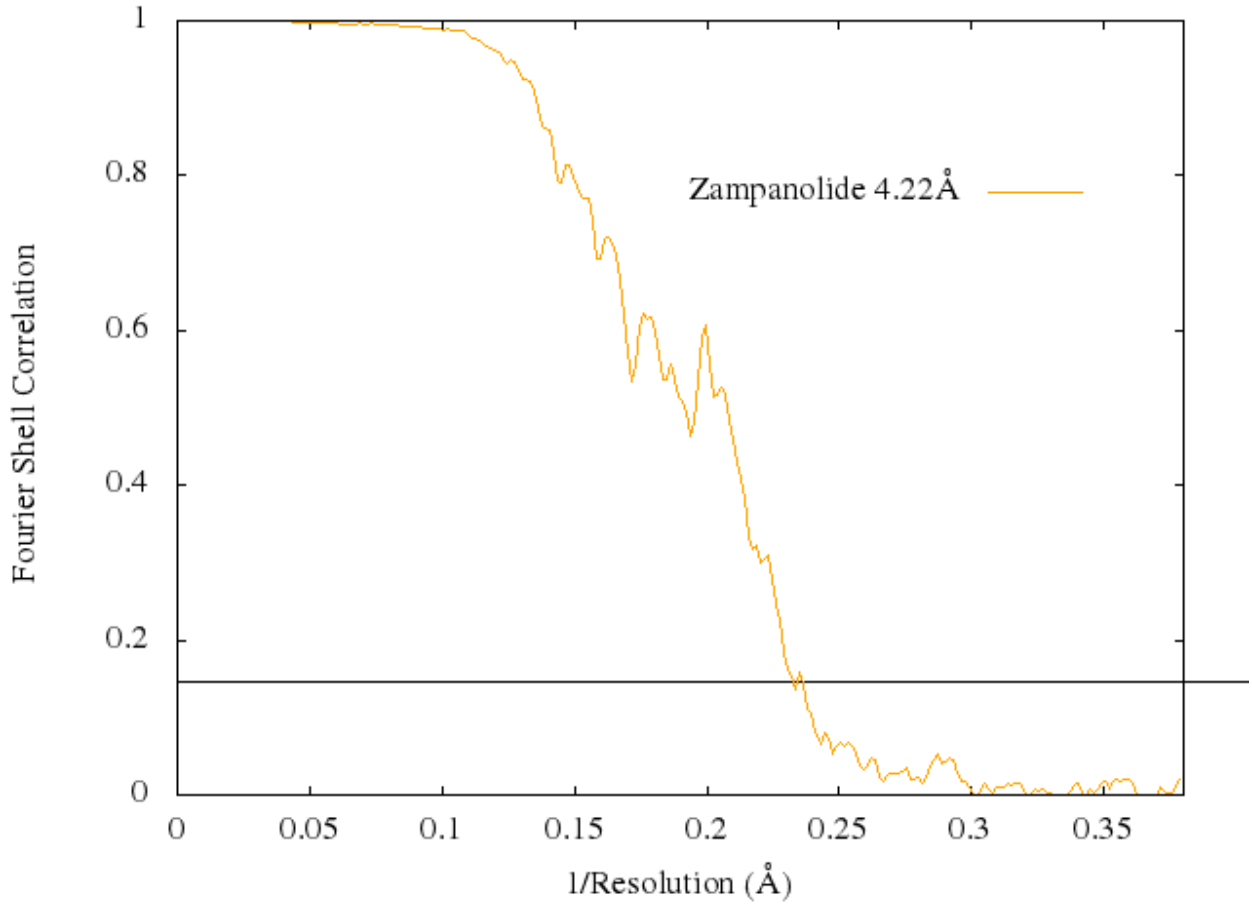

B)

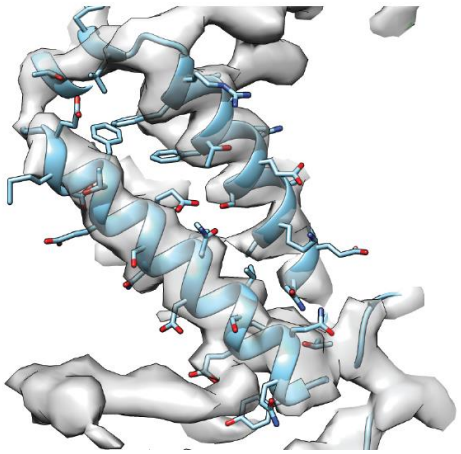

C)

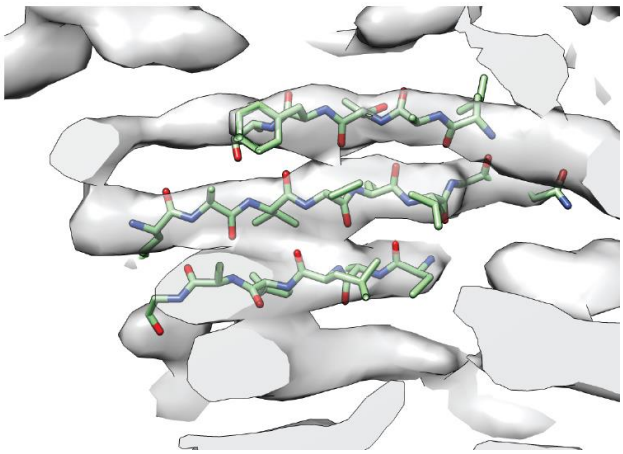

Figure 2.4 : High-resolution features in a MT cryo-EM map. Fourier Shell Correlation (FSC) and cryo-EM reconstruction with atomic model for the zampanolide-bound MT, showing separation of beta strands and helical pitches. α-tubulin is in blue and β-tubulin is in green.

The zampanolide reconstruction reached a lower resolution than has been obtained with some other MT samples using the same number of particles (22,000 particles). We attribute the resolution limitation to flexibility of the MT lattice, which seems to be induced by both zampanolide and Taxol. While the zampanolide-ligand envelope is defined (Figure 2.3) and sidechain density is observed, some features are lacking. This observation was also true for the Taxol-MT reconstruction (Elizabeth Kellogg, manuscript in preparation). It is common that a range of resolutions is observed within a single cryo-EM reconstruction. This is especially prevalent in the presence of flexible regions in a protein or if the sample lacks compositional uniformity. Calculating the local resolution of EM-reconstructions is commonly used to identify such regions. To address the limited resolution we encountered when analyzing zampanolide-bound MTs, we performed local resolution analysis on our reconstructions; similar analyses were done for Taxol-bound MTs (Elizabeth Kellogg, manuscript in preparation).

Our analysis showed that in the presence of zampanolide or Taxol (Elizabeth Kellogg, manuscript in preparation) a different local resolution distribution is obtained than for drug-free reconstructions. Surprisingly, the resolution for the motor domain of kinesin for zampanolide-MTs and Taxol-MTs (Elizabeth Kellogg, manuscript in preparation) is significantly lower (5-6 Å) (Figure 2.5 C) than that for tubulin (3-4.5 Å). To test whether the lower resolution for the kinesin is due to partial occupancy of kinesin along the MT, we calculated the kinesin occupancy. The kinesin occupancy estimates for the zampanolide-bound MT is $\geq$ 86% and $\geq$90% for Taxol-bound MTs. This suggests that the attachment of kinesin used in this study is either more flexible for the zampanolide- and Taxol-bound MTs, or that this is an alignment error that was propagated through the structure due to the helical arrangement flexibility. The importance of understanding how different MSAs affect MAP binding to MTs is highlighted by this discovery, given that most MAP-MT structural and biophysical studies are done with MTs bound to a MSA, with Taxol-MTs being the most frequently used.

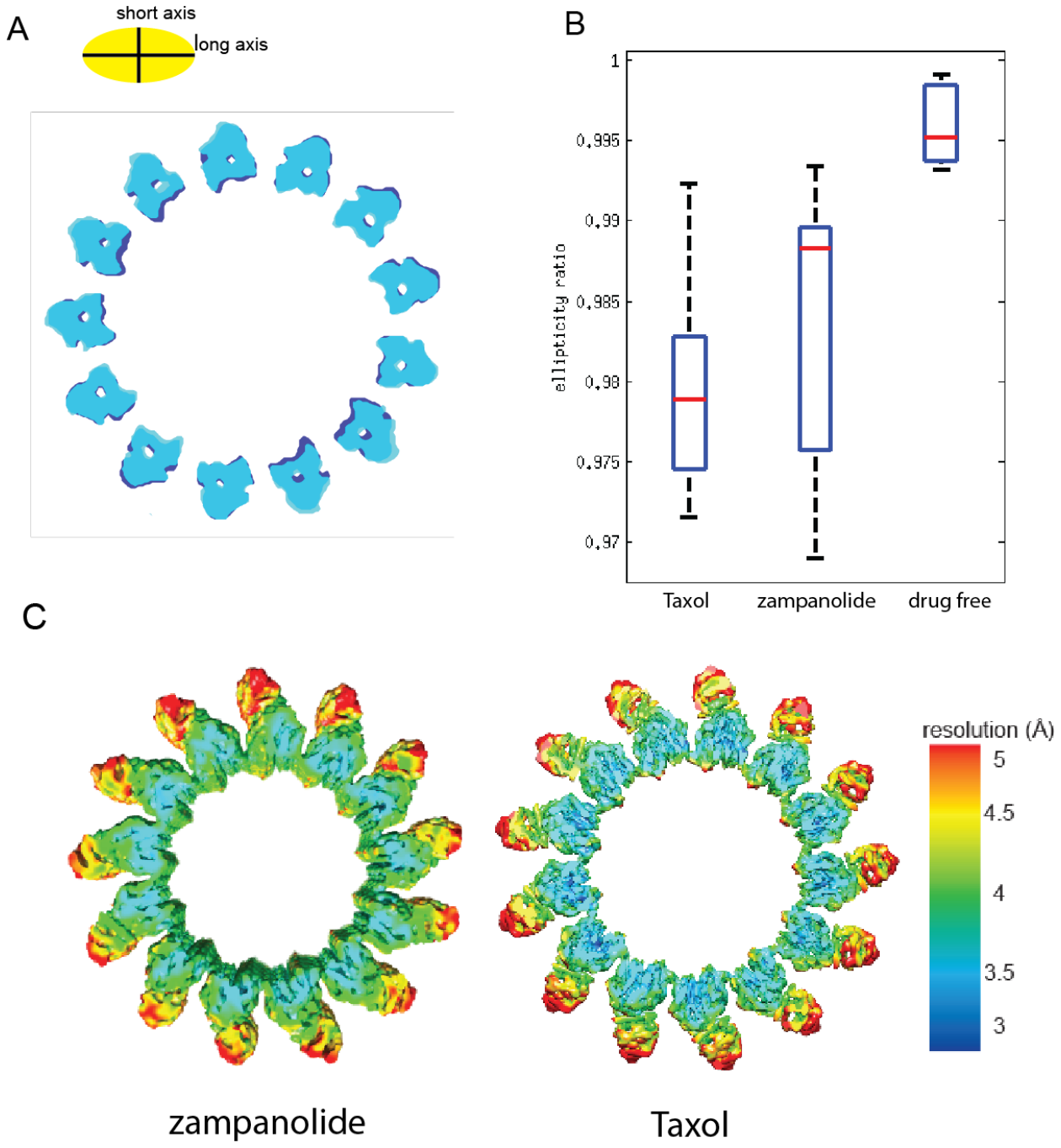

Figure 2.5: Zampanolide and Taxol induce MT wall flexibility. A) End-on view of two representative MT classes obtained from the Taxol-bound MT sample using RELION 3D sorting. B) The deformations from a circular cross-section were approximated as ellipses, and the parameters of the elliptical fits to the different 3D classes are displayed as a ratio between the long and short axes of the ellipse, average ratios are depicted as red lines C) End-on view of the Cryo-EM reconstructions of zampanolide (left) and Taxol-bound MTs (right). The decorating kinesin, used as a fiducial for the alignment of αβ-tubulin dimers, is visualized at significantly lower resolution in the Taxol sample, likely due to the alignment errors resulting from wall deformations in the MTs. Taxol analysis provided by Dr. Elizabeth Kellogg

Taxol-site binding results in lattice heterogeneity

Since the relatively lower resolution of the decorating kinesin is not due to partial occupancy, we sought to test whether it is attributed to conformational heterogeneity in the MTs bound to zampanolide or Taxol. RELION 3D classification was used to analyze the combined zampanolide-MT dataset (22,000 particles) and Taxol-MT dataset (23,000 particles), as well as the drug-free MT dataset (Elizabeth Kellogg, manuscript in preparation). Both of the resulting TSB (zampanolide-MT and Taxol-MT) 3D classes had visible deformations in the MT walls that were not identifiable in the drug-free 3D classes (Elizabeth Kellogg, manuscript in preparation). To quantify deformation in the MT walls, 2D projections along the MT axis were obtained from the 3D RELION classes. We then computed the elliptical parameters for a set of coordinates representing the center of each protofilament in a MT. For a perfectly circular MT, the long-axis (x-axis) and short-axis (y-axis) are equal. Thus, ration of the y-axis to the x-axis should equal one (Figure 2.5B). However, the TSB 3D classes show a wide range of 'elliptical' deformations in the microtubule walls (Figure 2.5 A-B) that correspond to ~1-2 Å displacement in the position of tubulin subunits. The 3D classes for drug-free MTs cluster together (Figure 2.5 C) suggesting a more homogenous population with more circular elliptical parameters suggesting that drug-free MT walls are less deformed than MTs bound to TSB MSAs.

To insure that the deformations we observe in the presence of TSBs are intrinsic to drug binding and not to MT flattening due to thin ice, we measured correlation between the deformed Taxol-MT segments within the 3D classes and image location on the grid (Elizabeth Kellogg, manuscript in preparation). If the deformations in the MT walls are induced by thin ice, we should observe a correlation between the image location and the deformed 3D class. Our analysis did not show any such correlation between deformed 3D classes and datasets or local regions on the grids. This indicates that the deformations in the MT walls are intrinsic to the binding of TBS MSAs and are independent of the structure of the drug. Despite our efforts to find a deformation-free subset for zampanolide-bound MTs, we were unable to find a class without such deformation. Subsequently, we were unable to improve the resolution of our cryo-EM map beyond the reported 4.2Å. The deformations in the MT walls that result from TSBs seem to be of a continuous nature and cannot be further characterized. Taxol-bound MTs exhibit the same characteristics as zampanolide, whereas peloruside, an MSA that binds to a location distinct from TSBs does not induce such heterogeneity (Elizabeth Kellogg, manuscript in preparation).

Taxol-site binders share common tubulin interactions

The zampanolide-tubulin complex has previously been studied in the context of unassembled tubulin (Prota et al. 2013). Here, we re-examine the modeled interactions between zampanolide and the microtubule in the context of our cryo-EM reconstruction. In the following section, the functional groups of zampanolide and Taxol are referred to by numbered carbon atoms (Figure 2.1). Due to MT-wall heterogeneity and sheet formation induced by the presence of zampanolide, our zampanolide-MT reconstruction is lower in resolution (4.2 Å) than the recently reported drug-free MT reconstructions (3.5 Å) (Zhang et al 2015) and slightly lower than Taxol-bound MT reconstruction (3.9 Å; Elizabeth Kellogg, manuscript in preparation). Despite the limited resolution of the zampanolide-MT reconstruction, a clear density corresponding to zampanolide is visible, and its binding location is in agreement with the crystal

structure (Prota et al. 2013). Density for the full ring is not present except at low isosurface thresholds (Figure 2.3), which could be due to inherent flexibility of the C1-C4 segment (Larsen et al. 2013). Mass spectrometry has shown that zampanolide interacts covalently with β-tubulin (Field et al. 2012). The covalent interaction was confirmed by the crystal structure, where the C-9 atom of zampanolide was shown to covalently bind to H7 of β-tubulin via H230. In addition, the crystal structure identified two hydrogen bonds between O1 atom of zampanolide and OH20, and the main chain carbonyl oxygen and the NH group of T277 respectively (Prota et al., 2013). Our cryo-EM reconstruction shows that zampanolide makes specific contacts with β-H230 (through covalent bonding) and β-T277 (through hydrogen-bonding interactions with the N-acyl hemiaminal group of zampanolide) (Figure 2.6) which is in agreement with what was previously reported. Furthermore, our data shows that zampanolide does not directly interact with the M-loop in the context of a polymerized MT. The location of the M-loop in our density map is different than in the crystal structure but it is consistent with the helical parameters obtained for zampanolide bound MTs (the supertwist).

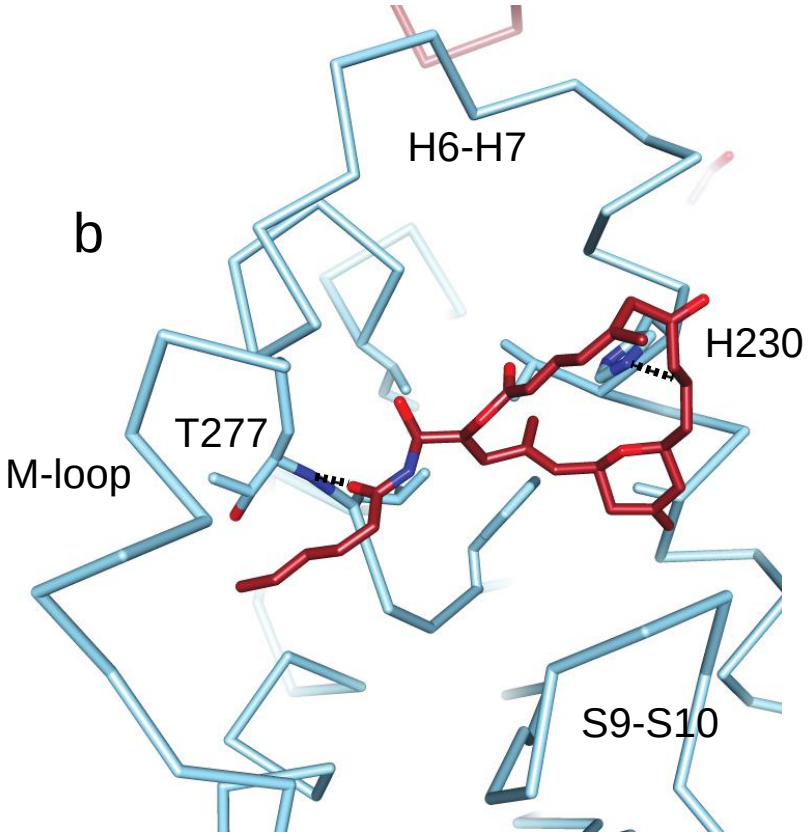

Figure 2.6: Atomic model of the zampanolide-binding pocket in zampanolide-bound MTs. The two major tubulin-zampanolide interactions are shown by dashed lines.

The highest resolution EM map of Taxol-bound MT (Elizabeth Kellogg, manuscript in preparation) defined three critical interactions between tubulin and Taxol; a van der waals interactions between the 2'-phenyl of Taxol, which has been previously shown to be essential for Taxol's stabilizing activity (Sharma, Lagisetti et al. 2013), and β-tubulin H230 (Figure 2.3 &

Figure 2.7). Additionally, the nitrogen in β-H230 is appropriately positioned to make a hydrogen bond with Taxol's 3'-oxygen. In addition, Taxol's 2'-OH is close enough to hydrogen-bond with the backbone carbonyl of R359. The final interaction involves the β-tubulin backbone NH of T277 (in strand S7) making a hydrogen bond with Taxol's oxetane ring, a Taxol group that has also been shown to be critical to its stabilizing activity (Elizabeth Kellogg, manuscript in preparation). The C13 sidechain of Taxol is found to interact with helix H7 and provides hydrophobic contacts, particularly with β-H230, furthermore, the map density does not support direct contacts between Taxol and the M-loop (Figure 2.7).

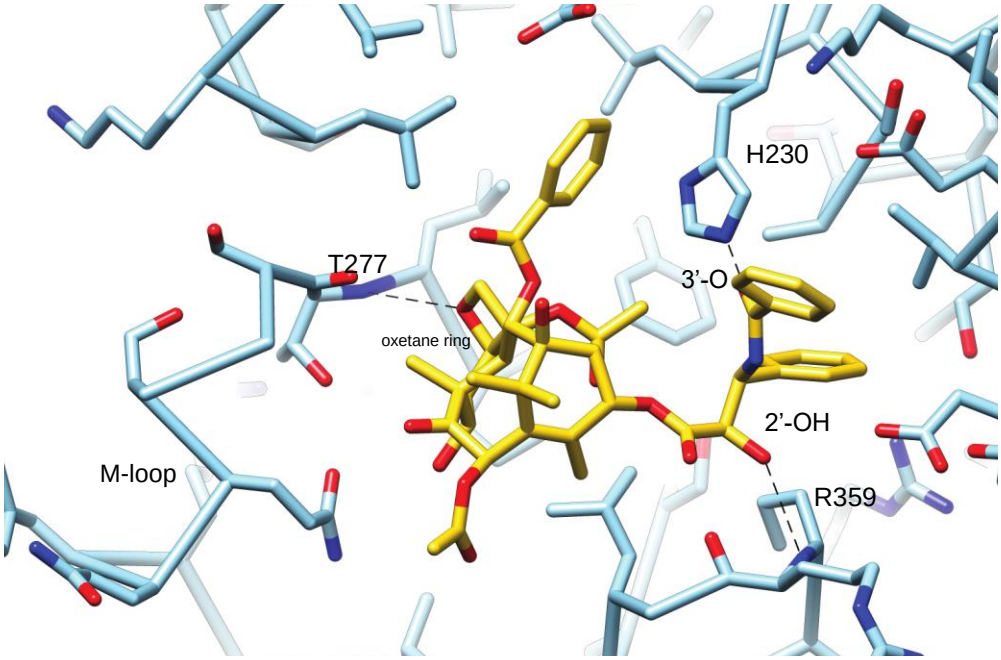

Figure 2.7 : Atomic model of the Taxol-binding pocket. Three critical tubulin-Taxol interactions are depicted by the dashed black lines (Elizabeth Kellogg, manuscript in preparation).

Taxol-site binders have different effects on the Taxol-site binding pocket

To analyze the effects of zampanolide and Taxol on the Taxol-binding pocket we compared the refined atomic models that we generated from MTs complexed with each drug. To assess relative fit of atomic models within density maps, Fourier-Shell Correlation (FSC) was computed between a simulated map (using the atomic coordinates) against the experimental map, with values closer to one indicating better correspondence with the experimental density. The Taxol-model fits the Taxol-map the best (0.81) whereas the drug-free model fits slightly worse (0.75) (Elizabeth Kellogg, manuscript in preparation) and zampanolide-MTs the least well (0.72), supporting our lattice-parameter measurements and indicating that the Taxol-MT and zampanolide-MT models are more divergent with respect to one another than to the drug-free state. A different trend is observed when using the zampanolide-MT reconstruction as a reference, but this may be due to the higher resolution of the map used for refinement (Taxol-MT

map vs zampanolide-MT map, 3.9 Å vs 4.2 Å) and the resultant higher quality of the Taxol-MT model.

Taxol-binding appears to give rise to subtle changes in the loops surrounding the binding pocket with respect to the drug-free atomic model, most significantly in the S9-S10 loop (0.53 Å Cα rmsd) which is moved down towards the N-site (Figure 2.8), the M-loop towards Taxol, and the H6-H7 loop away from the Taxol ligand (Elizabeth Kellogg, manuscript in preparation). In contrast, zampanolide-binding seems to result in a different response; the S9-S10 loop appears to close inward slightly and the M-loop adopts a 'pushed out' position with respect to both the drug-free model and the Taxol-bound model. This indicates that while the two TSBs make similar contacts with tubulin, the markedly different structures of the TSBs Taxol and zampanolide result in different structural responses in the vicinity of the binding-pocket.

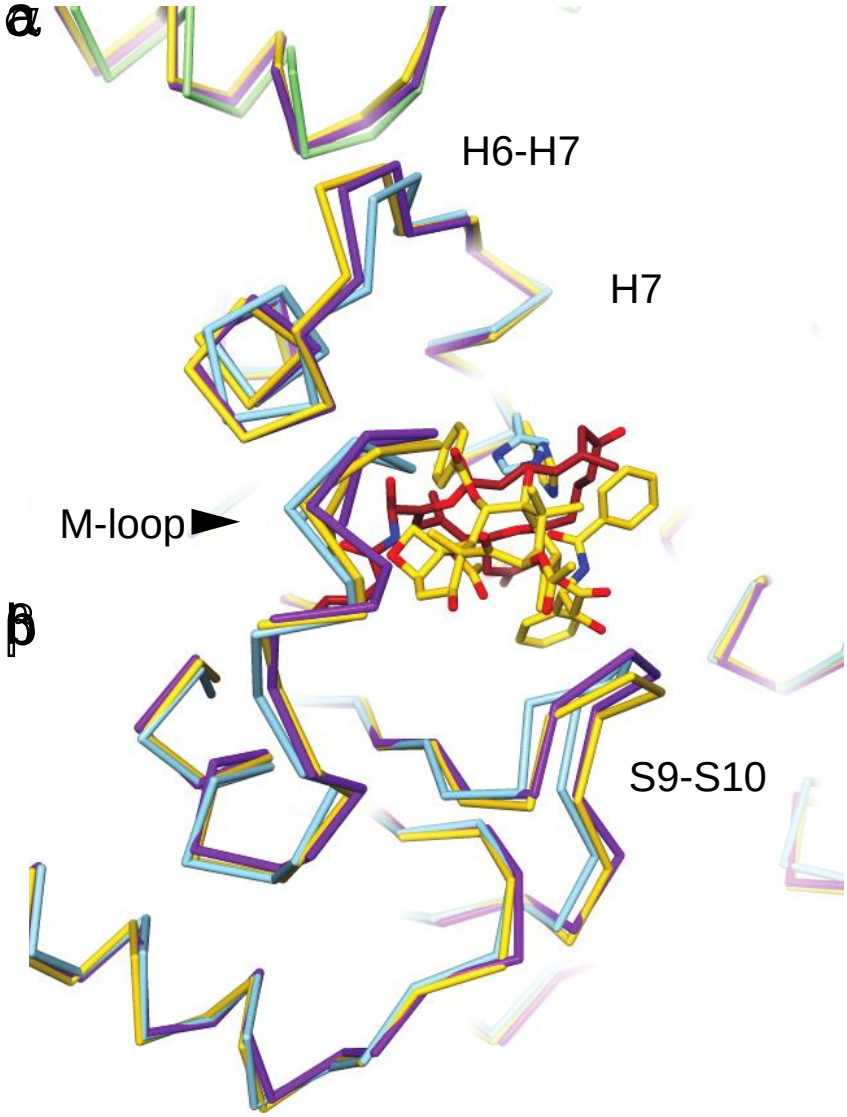

Figure 2.8: Comparison of the Taxol and zampanolide binding pockets. Superposition of the refined atomic models for Taxol-bound (gold), drug-free (purple) and zampanolide-bound (blue and green) MTs

Discussion

Our studies demonstrate that the TBS MSAs zampanolide and Taxol have distinct effects on the MT lattice. Using 3D classification, we have identified structural heterogeneity that is observed in the present of zampanolide and Taxol. This structural heterogeneity seems to result from the continuous deformation of the MT walls upon the binding to zampanolide or Taxol. The wall flexibility limits the resolution of our cryo-EM maps rendering further data interpretability difficult. We interpret this flexibility induced by zampanolide and Taxol to be inherent to the stabilization mechanism by TSBs. We infer that TSBs result in freeing the lateral contacts allowing them to adopt a wider range of conformations, subsequently enabling the MTs to tolerate lattice defects and resist disassembly. Upon binding, zampanolide and Taxol share two critical contacts with β-tubulin namely, a hydrogen-bond to the nitrogen backbone of T277 (immediately preceding the M-loop) and a critical interactions with H230. The functional groups that form these contacts are known to be critical for microtubule-stabilizing activity. Neither zampanolide nor Taxol form a direct contact with the M-loop in the context of a MT lattice.

While zampanolide and Taxol share more in common than their binding pocket in the lumen of a MT, they affect MT lattice parameters differently. Taxol has been previously reported to straightening of the protofilaments (Elie-Caille et al. 2007), indicating that it results in an allosteric structural change at the E-site. Unpublished work by Dr. Elizabeth Kellogg had confirmed that Taxol expanded axial repeat (Elizabeth Kellogg, manuscript in preparation). Strikingly, zampanolide did not result in an expanded lattice like Taxol. In the presence of zampanolide, MTs have a highly compressed lattice and a negative helical supertwist. The structural changes of the Taxol-binding pocket show that in the presence of Taxol, the binding pocket is "expanded", pushing the S9-S10 loop and H6-H7 loop away (Elizabeth Kellogg, manuscript in preparation). On the other hand, zampanolide-binding causes the movement of the M-loop as well as differences in the S9-S10 loop and H6-H7 loop that results in 'closure' of the Taxol-site pocket. This seems to be due to the distinctly different molecular shape of zampanolide itself. The lattice parameter measurements we have for zampanolide- and Taxol-bound MTs are in agreement with the changes we see in the binding pocket, and suggests that, as proposed previously (Prota, Bargsten et al. 2013), zampanolide may affect lateral contacts more than longitudinal contacts, whereas Taxol has the opposite effect.

The heterogeneity induced by the addition of TSBs to microtubules is of relevance to MAP studies. Taxol is commonly used as a stabilizing drug for microtubules, especially for structural studied of motor proteins and other MAPs. The heterogeneity observed in our 3D classes would always result in limited resolution for structural studies, and thus, using other MSAs that do not induce heterogeneity is recommended. Non-TSBs, such as peloruside, do not exhibit heterogeneity (Elizabeth Kellogg, manuscript in preparation) and might be more suitable for structural studies.

Our findings that zampanolide and Taxol have distinct effects on the MT lattice, suggest that there are multiple ways in which the MT can be stabilized against disassembly, even among MSAs that bind to the same pocket in the tubulin dimer. My work on zampanolide and Dr. Elizabeth Kellogg's findings on Taxol highlight the exquisite and complex structural responses of the microtubule-lattice to small differences in small-molecule structure. In this study we have speculated on potential models by which TSBs structurally affect the MT lattice, and more work is needed to test our ideas. The most severe obstacle we faced during this study was the inherent heterogeneity induced by TSBs and the flexibility of the MT walls in the presence of these drugs.

We were unable to sort this heterogeneity due to limitations in the currently used data analysis methods. Some groups are currently developing algorithms specialized in dealing with heterogeneity in helical filaments, such as frealix (Rohou & Grigorieff 2014). Our study has provided much needed insights into the stabilizing mechanism of TSBs; future work is certain to provide more of the mechanistic details that produce MT stability.

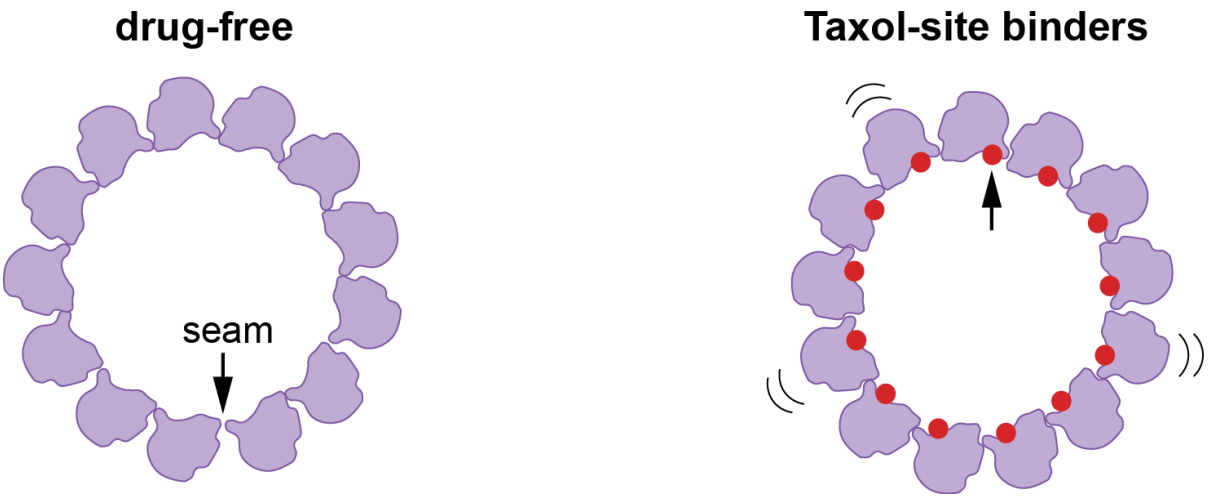

Figure 2.9: Schematic summary of changes in MT structure induced by TSB MSAs binding. Taxol and zampanolide induce lattice heterogeneity

Chapter Three: New insights into Tau's molecular mode of action using Cryo-EM

Introduction

Microtubules (MTs) are hollow elements in the cytoplasm of all eukaryotic cells. They play a pivotal role in vital cell functions including cell division, morphogenesis, and intracellular transport. MT dynamics are carefully controlled in vivo by several factors, among which is a family of proteins known as microtubule associated proteins (MAPs). Tau constitutes greater than 80% of total neuronal MAPs where it promotes the polymerization and stabilization of axonal tubulin and is necessary for neurite outgrowth (Garcia & Cleveland 2001).

In human brain, tau exists in six isoforms that result from alternative splicing of a single gene, MAPT (Aizawa et al. 1990). The isoforms, ranging in size between 352 and 441 amino acid residue, are developmentally regulated (Kosik et al. 1989) and differ by having either 3 or 4 semi-conservative repeats (with repeat 2 being the variable repeat) in the microtubule-binding domain near the carboxyl terminal, and in the presence or absence of two N-terminal inserts (Goedert et al. 1989) (Figure 3.1). There is evidence that the inter repeat (IR) regions can also bind to MTs (Goode & Feinstein 1994, Al-Bassam et al. 2002). The microtubule binding domain is preceded by a proline rich region (P1 and P2) and followed by a repeat-like domain (R'), both of which play a role in microtubule binding and assembly (Gustke et al. 1994; Goode & Feinstein 1994; Goode et al. 1997) (Figure 3.1). All four MT binding repeats have been shown to bind to and stabilize MTs independently, but the affinity of binding and the ability to stabilize MT increases with the number of repeats and the IR regions (Goode et al. 2000, Al-Bassam et al. 2002).

Tau has been predicted by some to be an intrinsically disordered protein, lacking any elements of secondary structures (Voter & Erickson 1982; Schweers et al. 1994). Other studies indicated that microtubule binding domain of tau could adopt a helical structure upon association with MTs (Eliezer et al. 2005). Tau's hyperphosphorylation at specific sites or mutation promotes dissociation from microtubules and leads to the formation of paired helical filaments (PHFs), the hallmark of a class of neurological diseases known as tauopathies (Biernat et al. 1993). The binding location of tau on microtubules and the stoichiometry of its binding have been controversial. Electron microscopy (EM) and undecagold labeling have been previously used to study the localization of tau on MTs. Tau has been reported to bind along protofilaments when added to pre-formed MTs (Al-Bassam et al. 2002) and inside the lumen of microtubules near the Taxol-binding site if tubulin is polymerized in the presence of tau (Kar et al. 2003). NMR studies have reported that tau binds at the interface between heterodimers (Kadavath et al. 2015). In addition, the tubulin C-terminus has been shown to participate in tau binding on the MTs, since the removal of the tubulin C-terminus by subtilisin is reported to reduce tau binding (Pashal et al. 1989, Serrano et al. 1985). Despite decades of research, the molecular mechanism of the tau-microtubule interaction which leads to microtubule assembly and stabilization is still unknown. We sought to take advantage of recent advances in direct electron detectors and data processing algorithms to study the direct interaction between tau and MTs via high resolution cryo-EM. With these advances we have obtained greatly improved resolution that allows much more precise understanding of the tau-MT interaction. We show that FL-tau binds on the surface of the microtubules along the protofilaments and we identify regions on tubulin that interacts with tau. We also use minimal tau constructs that contain either 2 or 4 repeats and bind similarly to FL-tau to refine the binding model. In addition, we found that FL-tau and minimal tau

constructs result in a MT lattice compaction. Our findings indicate that tau could result in MT stability by reinforcing the interdimer interactions along individual protofilaments in addition to sequestering the negatively charged tubulin C-terminus.

Materials and Methods

Tau purification

Full length tau (FL-tau) plasmid was a gift from Dr. Michael Ehrmann, University of Duisburg-Essen. The cloning of the repeat constructs was done by the UC Berkeley QB3 MacroLab. Recombinant human tau constructs were expressed in *E. coli* BL21 DE3 RIL Codon+ from pET3d expression plasmids and purified as described (Tennstaedt el al. 2012) by Simon Poepsel, UC Berkeley.

Microtubules Binding Assays

Lyophilized porcine tubulin (Cytoskeleton Cat# T240) was suspended to 10mg/ml in EM buffer (80mM PIPES pH 6.8, 1mM EGTA, 1mM $MgCl_2$) supplemented with 10% glycerol and 1 mM GTP. For binding assays, Taxol stabilized microtubules were used. Taxol (Cytoskeleton Cat #TXD01) was resuspended in DMSO to create a 2 mM stock solution. Tubulin (10 aliquot) was allowed to polymerize for 15 min at 37 °C before adding 2 µl of 2mM Taxol. MTs were spun at 17,000 g for 20 minutes using a tabletop centrifuge. The MT pellet was resuspended in 30 µl EM buffer containing 133 µM Taxol to maintain Taxol:tubulin ratio. The tubulin concentration was estimated to be 70.7 µM. Equivalent molar amounts (3 µM) of tubulin and tau constructs were mixed to a final reaction volume of 40 µl. Negative controls were prepared by using equivalent volume of EM+Taxol "mock buffer" in place of tubulin to assess self-pelleting of tau constructs. MT-tau samples were incubated at 37 °C for 10 min before pelleting at 17,000 g for 20 minutes using a tabletop centrifuge. Supernatants (40 µl) were separated from the pellets and the pellets were resuspended in 4X SDS sample buffer containing 20 mM DTT and 20 µl EM buffer. The supernatant and pellets were heated at 95 °C for 10 min and the samples were loaded on denaturing Bolt™ 4-12% Bis-Tris Plus Gels (Invitrogen Cat#NW04120BOX). The gels were stained with SYPRO® Ruby Protein Gel Stain and imaged using (Bio-Rad Gel Doc© EZ Imager). Band intensities were determined using ImageJ.

Microtubule polymerization and vitrification

To prepare MTs decorated with FL-tau, porcine tubulin aliquots at 10mg/ml tubulin were diluted 4-fold into cold EM buffer supplemented with 10% glycerol (to mimic the buffer used to store tubulin at -80° °C), incubated on ice for 15 min, and then polymerized as usual. The dynamic microtubule pellet was resuspended in 20 µl warm EM buffer containing 1mM GTP. Tubulin was quickly diluted 5 fold in warm FL-tau (5mg/mL) to yield 0.5mg/ml tubulin concentration. A Mark V Vitrobot (FEI) was used to perform sample vitrification at 37 °C, and 100% humidity and a blot force setting of 10. Samples were prepared by incubating 2 µl of the MT:FL-tau mixture on holey carbon 1.2/1.3 C-flat grids (Protochips) for 30 seconds, then washing twice with 4 µl FL-tau construct, waiting 30 seconds between washes (total incubation

time: 2 minutes). To test if FL-tau and kinesin could simultaneously bind to MTs, we desalted kinesin as previously described (Alushin et al. 2015) and prepared grids similarly to the FL-tau but with an additional step. 2 µl of the MT:FL-tau mixture were incubated on holey carbon 1.2/1.3 C-flat grids (Protochips) for 30 seconds, then washed once with 4 µl FL-tau construct, and then with 4 µl kinesin, waiting 30 seconds between washes. Excess liquid was blotted and grids were plunged as usual.

A slightly different protocol was followed to prepare MTs decorated with 2-R or 4-R constructs to avoid formation of MT bundles. Tubulin aliquots (20 µl at 10mg/ml) were polymerized at 37 °C for 20 min and then spun at 17,000 g for 20 minutes using a tabletop centrifuge, and then resuspended in 24 µl warm EM buffer containing 1mM GTP. MT concentration was estimated to be 2.5mg/ml (~22.5 µM) by measuring absorbance at 280 via a NanoDrop. MTs were kept at 37 °C until ready to be used. To prepare cryo grids with 2-R and 4-R constructs, 2 µl of MTs were incubated on holey carbon 1.2/1.3 C-flat grids (Protochips) for 30 seconds, then washed twice with 4 µl of either tau construct, waiting 30 seconds between washes (total incubation time: 2 minutes).

To test if FL-tau binds inside the lumen of MTs, we co-polymerized tubulin in the presence of FL-tau as previously described (Kar, 2003). FL-tau was diluted to 1mg/mL (21.8 µM in EM buffer and heated to 55 °C for 5min. DMSO (5%) and 0.1M TMAO were added to tau before spinning it at 90K for 15min at room temperature. 1.5 µl of 20 mg/ml tubulin stock was mixed with 30 µl of 1mg/mL tau yielding a final tubulin concentration of 1 mg/ml (9.1 µM) . The tubulin was polymerized by incubating the mixture at 37 °C for 30 min. Kinesin was desalted as previously described (Alushin et al. 2014) and was used to decorate the outside of these MTs to aid in subsequent data processing. To prepare cryo-grids, 2 µl of MTs were incubated on holey carbon 1.2/1.3 C-flat grids (Protochips) for 30 seconds, then washed twice with 4 µl of kinesin, waiting 30 seconds between washes (total incubation time: 2 minutes).

Imaging and Post processing

Cryo-EM data collection proceeded as previously described (Zhang et al. 2015). A 300 kV Titan microscope (FEI) was operated at 27,500X magnification with a nominal pixel size of 1.32 Å. Prior to sample insertion, the gun-tilt and coma alignments were carefully performed. Images were collected in counting mode on a K2 Summit detector (Gatan), with a total dose of 27.5 e-/A^2. Each exposure was 6 seconds long and comprised a set of 20 frames of 300 ms exposure for each. Images were drift-corrected using UCSF motioncorr software (Bai et al. 2013), and particles (MT segments along the length of a MT) were boxed out using overlapping boxes, each box separated by either 80 Å, 160 Å or 320 Å along the filament with a box size of 512 pixels (~676 $Å^2$). CTFFIND4 (Rohou & Grigorieff 2015) was used to estimate CTFs for the drift-corrected images. The global alignment parameters were determined using a multi-reference alignment script (using EMAN2 libraries (Tang et al. 2007)), against low-pass filtered (~20 Å) references comprising 12-15 protofilament MT models. The resulting global alignment parameters were used as inputs for refinement in FREALIGN (Lyumkis et al. 2013) to obtain reconstructions of MTs bound to tau that reached 4.3-5.5 Å resolution. Pseudo-helical symmetry was imposed as previously described (Sindelar & Downing, 2007; Alushin et al. 2014) to generate a 'good' protofilament that was then used to create a full MT model for further refinement. The refinement was carried out for 3 iterations or until reconstruction resolution

converged. To accurately determine αβ-tubulin register and seam location for each MT segment, we utilized seam-search strategies previously described (Zhang et al., 2015).

Results

FL-Tau in the presence of MTs results in the formation of tubulin rings and sleeves

To investigate how tau stabilizes microtubules, we have analyzed the interaction between Taxol-MTs and human FL-tau using co-sedimentation assays (Figure 3.1). Little tau self-pelleting was observed in the absence of MTs. In the presence of MTs, the density of the FL-tau band for the pellet was higher indicating that FL-tau binds to MTs (Figure 3.1 B and C). Relative amounts of tau present in either the supernatant (S) or pellet (P) fraction were determined by dividing the intensity of the tau band for each fraction by the sum of tau intensities in both pellet and supernatant fraction of each sample.

$$Relative\ Intensity = \frac{Intensity\ of\ tau\ in\ a\ fraction}{Intensity\ of\ tau\ in\ pellet + intensity\ of\ tau\ in\ supernatant}$$

The co-sedimentation assay shows that even though tau co-sediments with MTs, a significant amount of tau remains in the supernatant. This indicates that tau has low affinity to MTs under this experimental set up. The stoichiometry of FL-tau was determined from gel band intensity to be 1 tau protein for each 3.6 tubulin monomers, which is similar to previously reported values (Al-Bassam et al. 2003, Gustke et al. 1994, Coffey & Purich, 1995).

A)

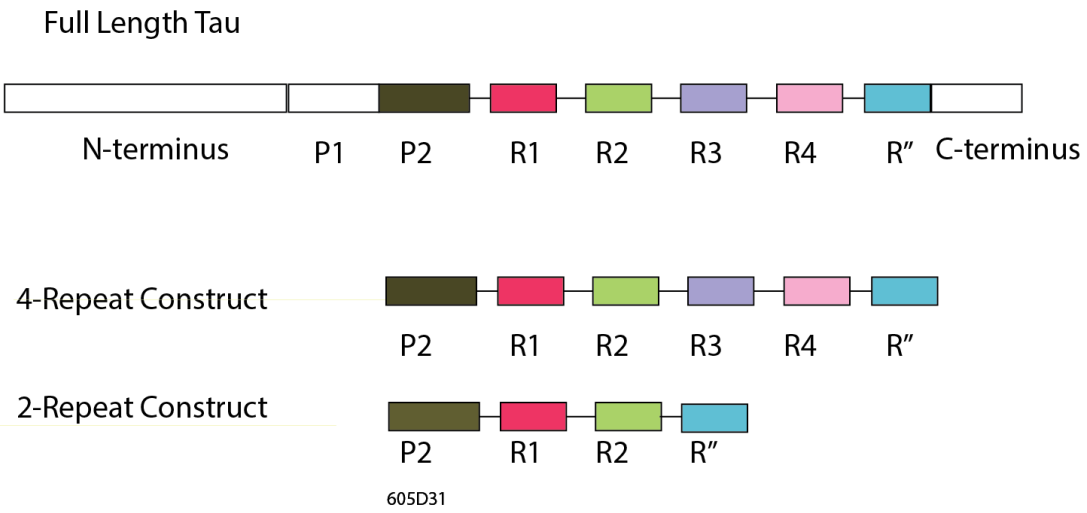

P2: 197 YSSPGSPGTPGSRSRTPSLPTPPTREPKKVAVVRTPPKSPSSAKSRL 243
IR1-R1: 244 QTAPVPMPDLKN-VKSKIGSTENLKHQPGGGK 274
IR2-R2: 275 VQI INKKLDLSN- VQSKCGSKDNIKHVPGGGS 305
IR3-R3: 306 VQIVYKPVDLSK- VTSKCGSLGNIHHKPGGGQ 336
IR4-R4: 337 VEVKSEKLDFKDR-VQSKIGSLDNITHVPGGGN 368
R″:369 KKIETHKLTFRENAKAKTDHG-AEIVYKSPVVS 400

B)

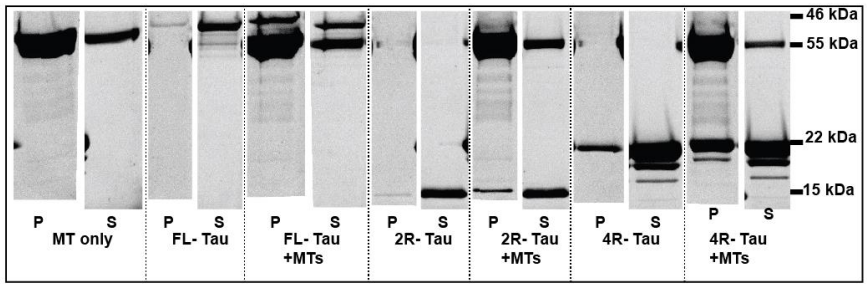

C)

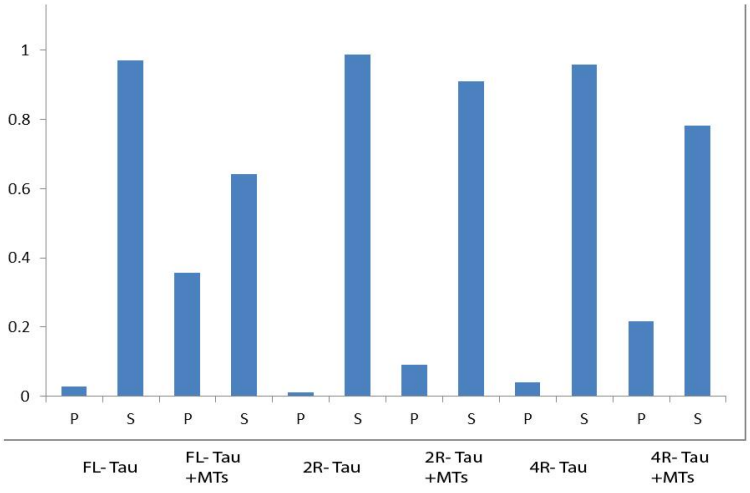

Figure 3.1: **FL-tau and minimal constructs bind to Taxol-MTs.** A) Schematic of tau constructs used in the study, the schematic is proportional to the size of each region in the FL-tau. Positively charged amino acids are underlined in each domain. B) Microtubule binding assay showing that all tau constructs bind to MTs, but with low affinity. C) Relative amount of tau present in the pellet and supernatant fractions.

When FL-tau was mixed with tubulin, MTs polymerization occurred below the normal tubulin critical concentration even with sub-stoichiometric amounts of tau as seen in our electron micrographs (Figure 3.2). This observation is in agreement with what has been previously reported (Goedert & Jakes, 1990). With sub-stoichiometric amounts of FL-tau, tubulin double rings were seen in the background (Figure 3.2 A) in addition to fully formed MTs. With saturating amounts of FL-tau, the double ring structures were no longer observed and most MTs decorated with FL-tau looked similar to naked MTs (Figure 3.2 B). Furthermore, adding FL-tau to dynamic MTs promoted tubulin polymerization and did not induce bundling (Figure 3.2 B), which is in agreement to previously reported data (Barnt et al. 1993). However, we observed sleeve-like structures forming around the polymerized MTs (Figure 3.2 C). The sleeve-like structure is only sparsely observed (below 5% of all MTs in the data set).

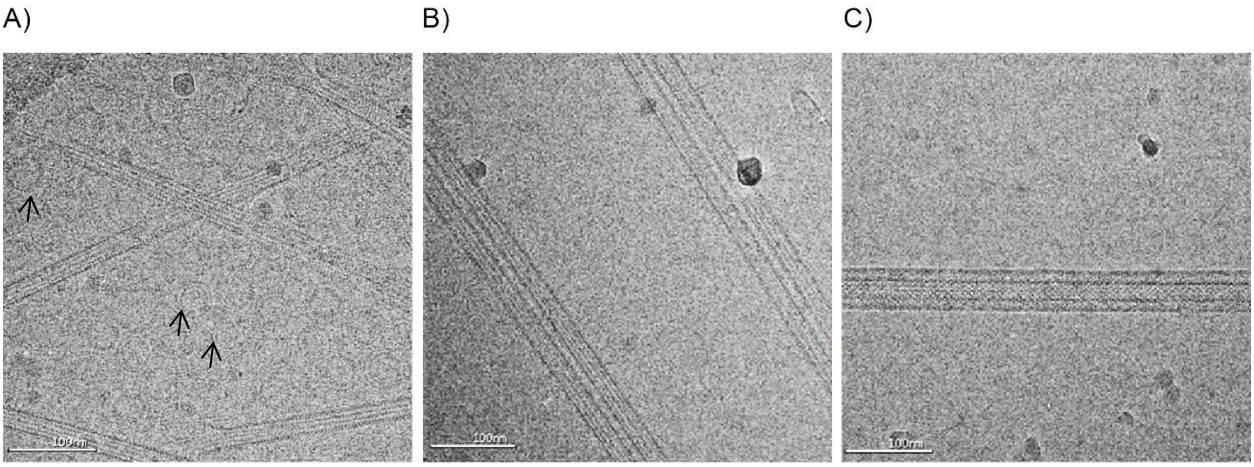

Figure 3.2: **Micrographs of FL-tau bound to MTs**. A) Tubulin double rings are formed at sub-stoichiometric amounts of tau. B) Double tubulin rings are no longer observed at saturating levels of tau. C) Sleeve-like structures were seen only occasionally in the presence of FL-tau.

FL Tau binds exclusively to the MT exterior, interacting with tubulin C-terminal helices

Our cryo-EM reconstruction of FL-tau shows extra density for the protein on the outside of MTs along the ridges of each protofilament (Figure 3.3). Our results show that most of the FL-tau is in an extended conformation when bound to microtubules, as would be suggested by previous structural studies (Al-Bassam et al. 2002). The improved resolution in our work allows a more precise interpretation of the binding pattern and structure of tau. The reconstruction of FL-tau bound to MTs shows that the interaction between FL-tau and MTs happens through extended regions of the tau protein that arranges itself longitudinally along each protofilament (Figure 3.3 A). The density corresponding to tau has few distinct features and seems to form a single continuous density along the MT surface. This may potentially be due to an artifact

introduced by our image-processing pipeline. Usually the particles that go into our reconstructions consist of MT segments that are separated by 80 Å along the MT filament. Using an overlap of 80 Å assumes that each tubulin dimer is an asymmetric unit, the smallest unit of volume that contains all of the structural information. Each asymmetric unit is assumed to contain identical image elements. Using an overlapping box size of 80 Å yields accurate reconstructions if each FL-tau molecule binds to a tubulin dimer. Using larger spacings of the boxes along the MT allows identification of larger repeat units, but results in fewer particles, which leads to a lower resolution MT reconstruction (Figure 3.4). Since our co-sedementation assay (Figure 3.1) and other reports suggest that FL-tau binds every 3.5 monomers, we attempted to eliminate artifacts due to overlapping boxes by processing MTs decorated with FL-tau using different box spacings, separated by either 80 Å (1 tau:tubulin dimer), 160 Å (1 tau:2 dimers, corresponding to stoichiometry determined by binding assays) or 320 Å (1 tau: 4 dimers) along the filament (Figure 3.3). Our reconstructions show that regardless of the way we process the MTs, FL-tau forms a continuous density that spans both α- and β-tubulin (Figure 3.3 D).

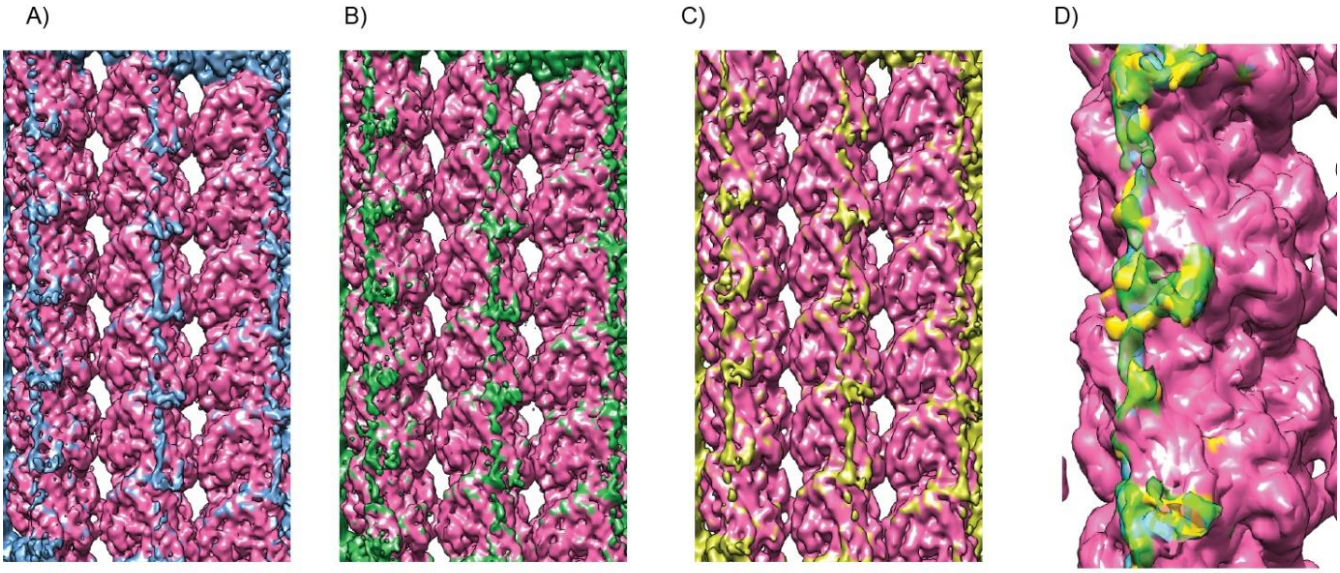

Figure 3.3: **Cryo-EM reconstructions of FL-tau constructs bound to MTs along each protofilament near the tubulin C-terminus.** A) FL-tau density is shown in blue; 80Å was used for box spacing B) FL-tau denisty is shown in green; 160 Å was used for box spacing C) FL-tau density is shown in gold; 320 Å was used for box spacing D) Close up of all reconstructions overlapped. In all panels, density corresponding to tublin is colored pink.

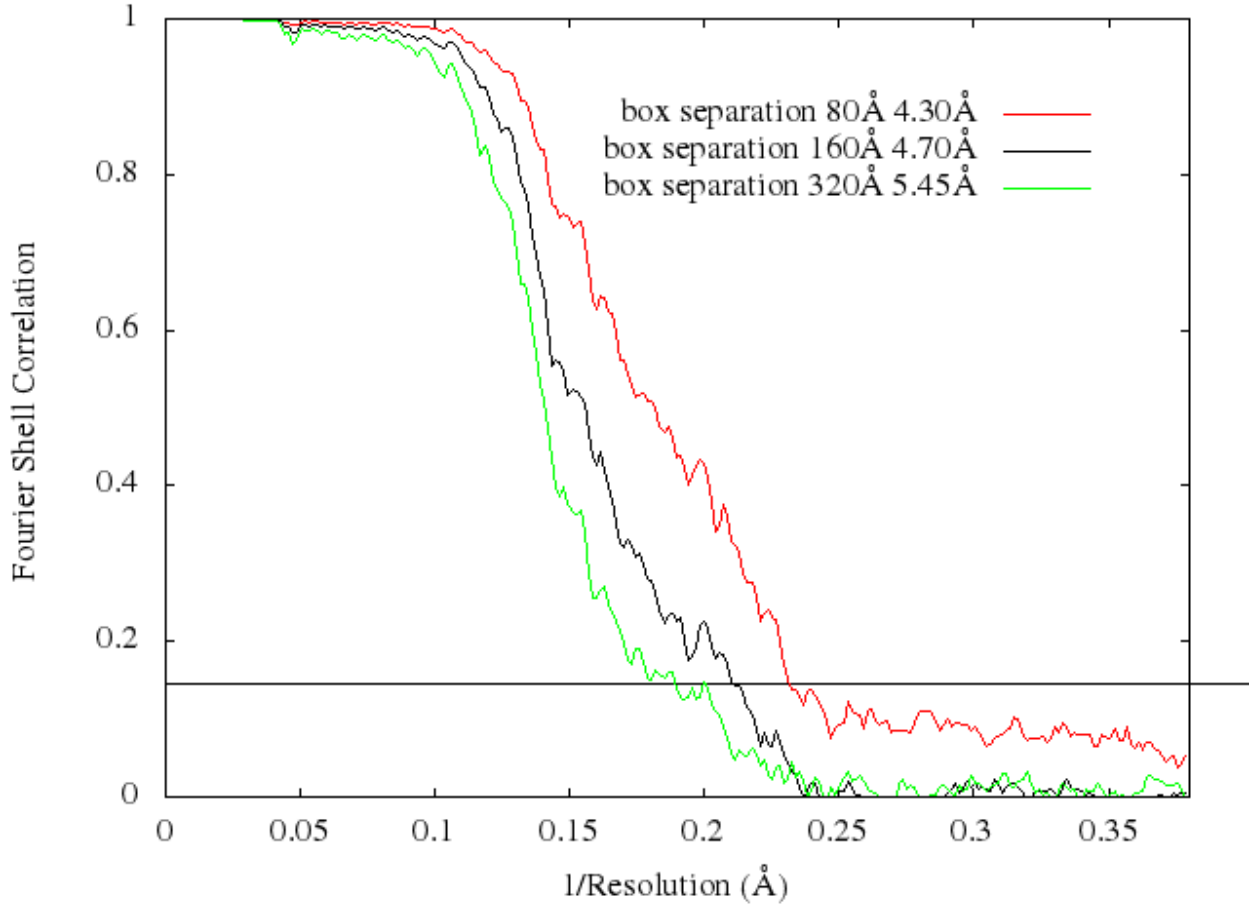

Figure 3.4: **Fourier Shell Correlation (FSC) for FL-tau reconstructions using different box spacings.**

The binding location of tau has been controversial, with the suggestion that tau could bind to a site inside the MT lumen when present during MT polymerization (Kar et al., 2003). To test whether FL-tau can bind inside the lumen of MTs we polymerized tubulin in the presence of excess amounts of FL-tau and collected cryo-EM data. Our reconstructions did not show any extra density inside the MT lumen that could be attributed to tau (Figure 3.5) as previously reported (Kar et al., 2003). The higher resolution of this work, along with the established data processing methods for MTs, gives us confidence that tau does not bind on the MT interior. Furthermore, the addition of kinesin to pre-formed MTs decorated with FL-tau results in the dissociation of tau from the microtubules surface (Figure 3.6). This result confirms that tau and kinesin bind to the same region on the surface of tubulin as previously suggested (Trinczek et al. 1999), and it shows that kinesin has stronger affinity to MTs in comparison to FL-tau.

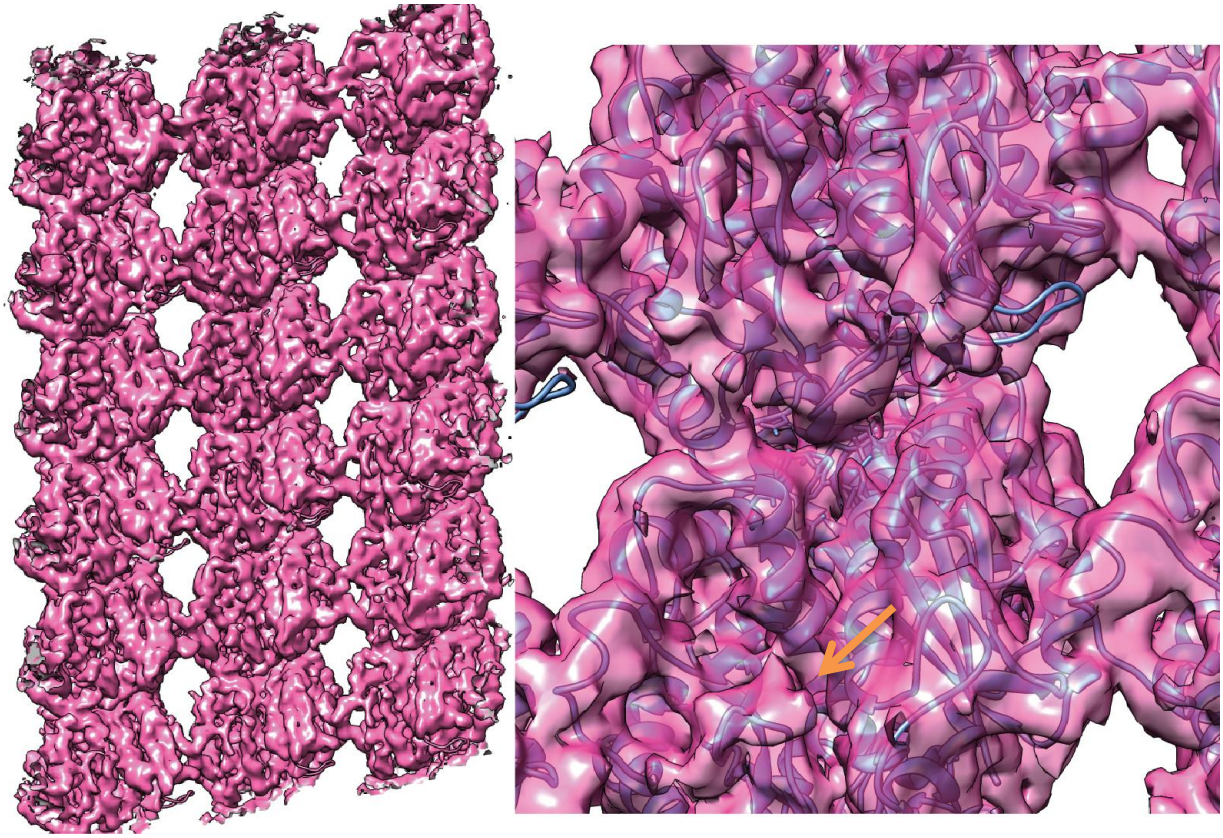

Figure 3.5: FL-Tau binds exclusivly an the oustide of MTs. The lumen of a MT that was polymerized in the presence of tau does not show extra density to account for tau binding. The arrow is pointing to the Taxol-binding pocket, where tau was proposed to bind.

A) B)

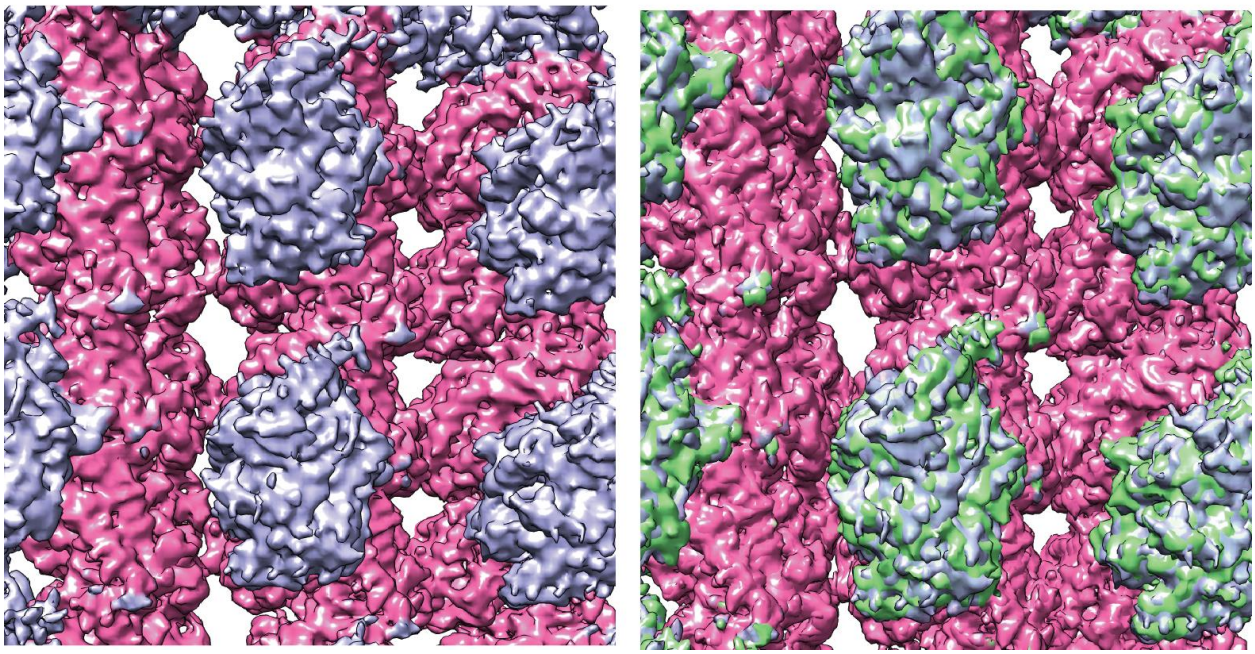

Figure 3.6: **Kinesin and FL-tau compete for MT binding.** A) Outer view of a MT that was decorated by FL-tau and then washed with kinesin shows that kinesin competes tau off the MT surface. Density that is not tubulin is in purple B) Overlay of panel A and a MT decorated with kinesin only (no tau). Density that is not tubulin is colored green.

Minimal Tau constructs function identically to full-length and have the same structure when bound to MTs

To gain deeper insights into tau tubulin interaction, we designed two minimal tau construct, designated 2-R construct and 4-R construct. 2-R construct contains the first two repeats of FL-tau whereas 4-R construct contains all 4 repeats (Figure 3.1 A). The repeat region of FL-tau binds to microtubules and promotes its assembly, but the repeat region alone binds with low affinity. In addition to microtubule binding repeats, our minimal constructs have a proline-rich region on the N-terminus and a repeat-like domain, R", on the C-terminus, both of which are known to enhance the binding to MTs (Gustke et al. 1994, Goode et al. 1997). Our binding assay shows that both 2-R and 4-R constructs bind to microtubules (Figure 3.1 B and C). The co-sedimentation assay shows that a significant amount of tau remains in the supernatant in the presence of excess tubulin, which indicates low binding affinity to MTs under our experimental setup (Figure 3.1 B). Our cryo-EM micrographs showed that in the presence of 2-R or 4-R constructs, tubulin polymerized below the critical concentration, in a manner comparable to the FL-tau (Figure 3.7). When the minimal constructs were mixed with dynamic MTs, sleeve-like structures formed around the polymerized tubulin, like those observed when FL-tau was added to MTs but more frequently. The sleeve-like structure is twice the diameter of a MT and the spacing between the sleeve-structure filaments was measured from micrographs to be ~50 Å, similar to protofilament spacing in a MT lattice, suggesting that these sleeve-like structures consist of tubulin dimers. The fast Fourier transforms (FFTs) of these decorations show a consistently strong 40Å layer line and an X-pattern (Figure 3.8) which varied for different MTs. The sleeve-like structure was infrequently observed in our micrographs when FL-tau and MTs were mixed (on ~5% of MTs) but it was abundant (over 65%) when 2-R construct was added to microtubules (Figure 3.7 A and B). In addition, the mixing of 2-R construct or 4-R construct and MTs in a tube resulted in MT bundling (Figure 3.7A). MT bundling in the absence of the N- and C-terminus of tau has been previously reported (Barnt et al. 1993).

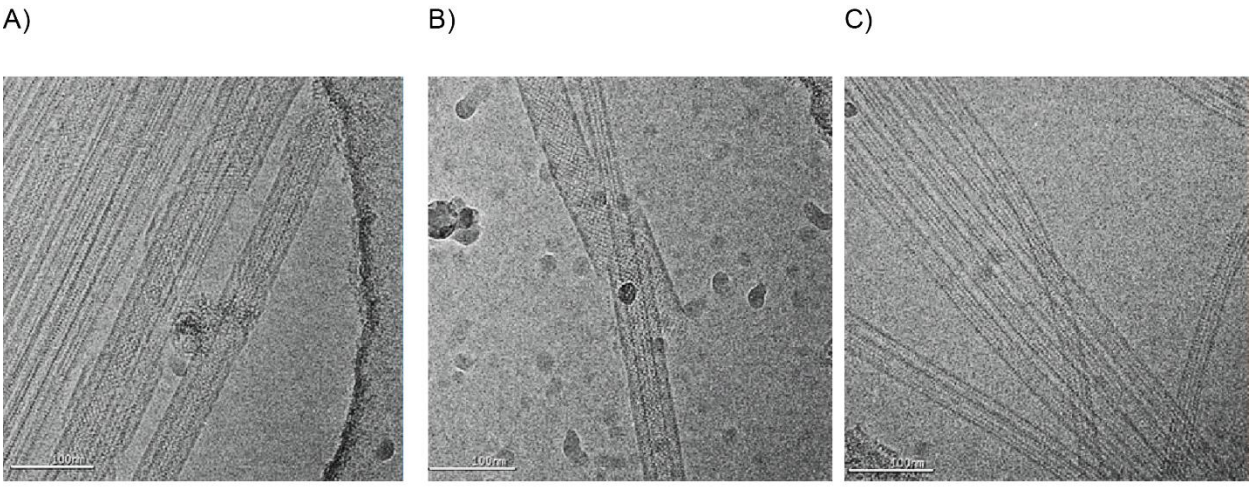

Figure 3.7: **Micrographs of 2-R construct**. A) Sleeve-like structures are frequently observed when 2-R construct was mixed with MTs in a tube. B) Sleeve-like structure forming C) Immobilized MTs that were subsequently decorated with 2-R show significant reduction in sleeve-like formation.

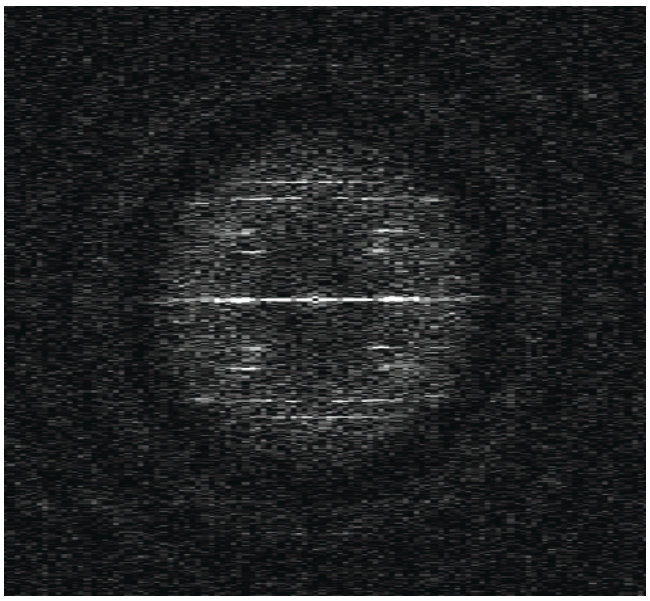

Figure 3.8: FFT of the sleeve-like structure showing a 40Å layer line and X-like pattern characteristic of a helical structure.

2-R construct is potentially in contact with over 12 aa near the tubulin C-terminus

Because 2-R construct seemed functionally identical to FL-tau in promoting tubulin polymerization and MT stability, we used it to identify the regions of FL-tau that are essential for tau interactions with MTs. To obtain high resolution cryo-EM reconstructions we avoided the formation of sleeve-like structures and MT bundling induced by 2-R by immobilizing dynamic MTs on carbon grids and washing them with 2-R constructs at high concentrations (10mg/mL) to insure full decoration. This method enabled us to collect sufficient data to obtain high resolution

reconstructions of 2-R tau construct bound to MTs. Our reconstruction of the 2-R construct bound to MTs shows that the 2-R construct binds along the protofilaments in a manner indistinguishable from FL-tau (Figure 3.9 A). MTs decorated with 4-R construct were prepared similarly and the reconstruction of 4-R construct bound to MTs was also indistinguishable from FL-tau and 2-R construct (Figure 3.9 B).

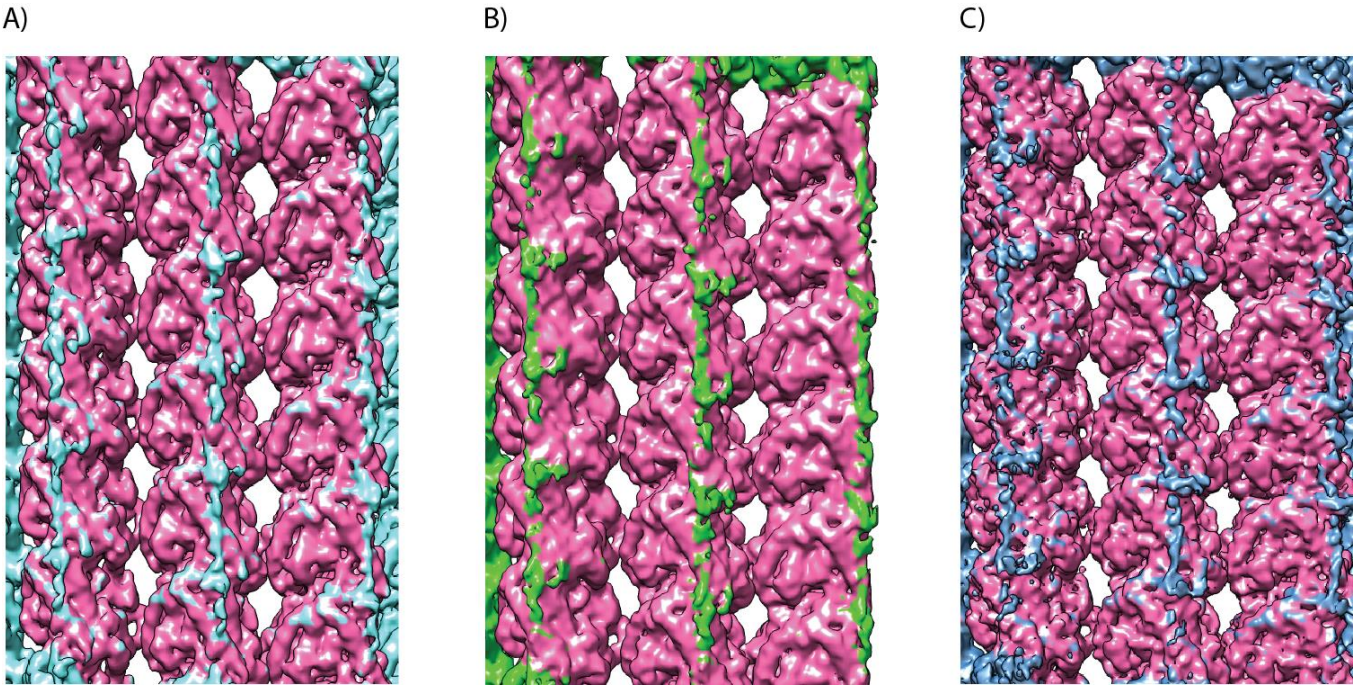

Figure 3.9: **MT reconstructions decorated with 2-R construct, 4-R construct and FL-tau**. A) Density of 2-R construct is shown in cyan B) Density of 4-R construct is in green C) Density of FL-tau is in blue. Tubulin is in pink.

The density map of 2-R construct bound to MTs was used to identify amino acid residues on the MT surface that are close enough to interact with the 2-R construct (Figure 3.10 A and B). Our analysis shows that 2-R construct interacts with more residues on β-tubulin than on α-tubulin. 2-R construct is in close proximity to ARG 400, ARG 401, GLU 422, ASN 426, ASP 427, SER 430, GLU 431, GLN 434 and TYR 435 on β-tubulin whereas it is in close proximity to ARG 402, TYR 399 and LYS 430 in α-tubulin (Figure 3.10 C and D). Most of the identified amino acids on the tubulin surface that interact with 2-R tau construct are charged; further identification of relevance and significance in binding to tau would require point mutation analysis coupled with computational modeling. Our density map of 2-R construct bound to MTs also shows that 2-R construct binding leads to further structuring of the acidic C-terminus of both tubulin monomers (Figure 3.10 B). Other MAPs, such as PRC1, structure the MT tail in a similar fashion (Nogales Lab, unpublished data).

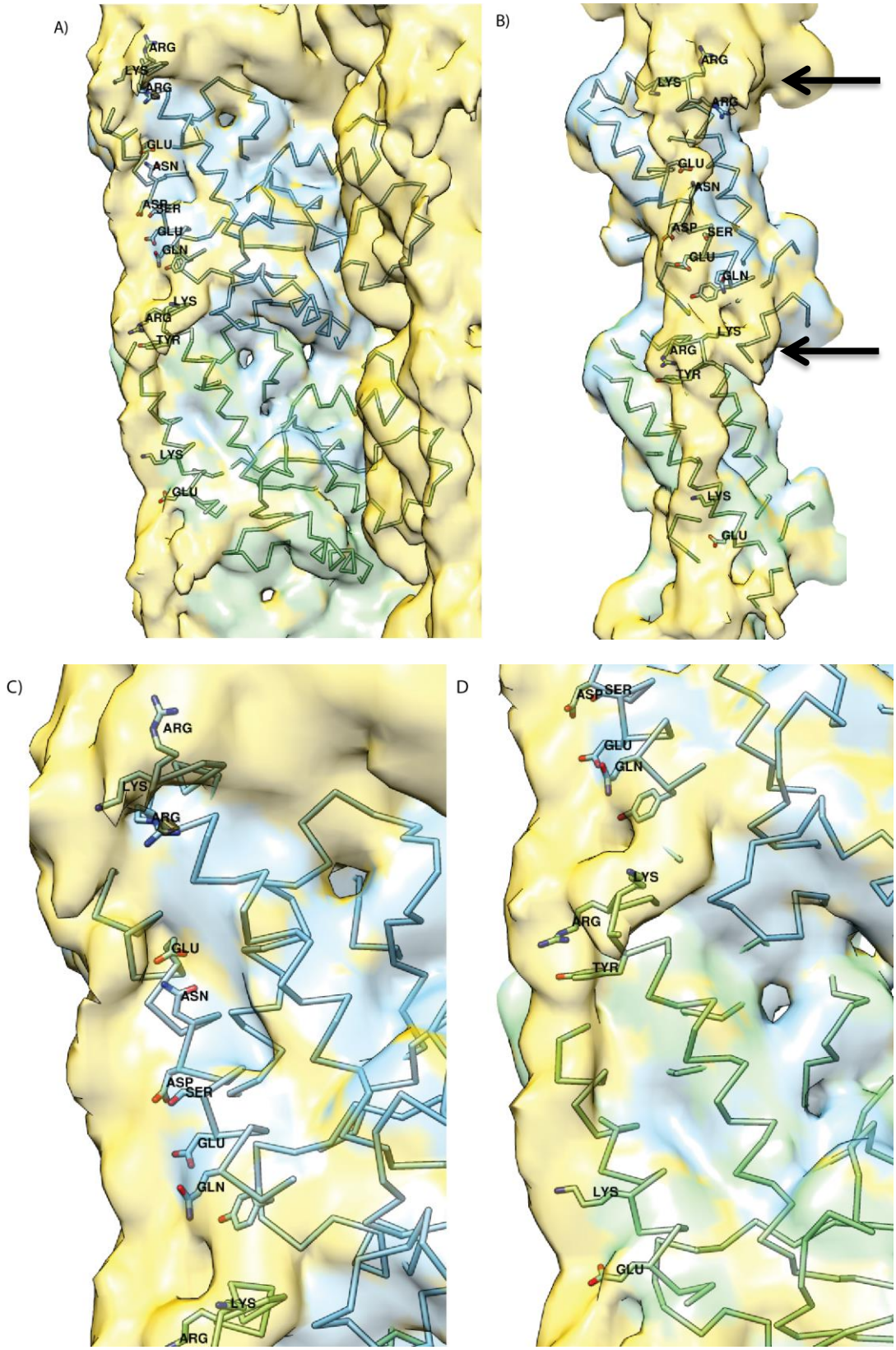

Figure 3.10: **2-R construct binds longtitudally along each tubulin dimer.** A) Side views of tubulin dimer decorated with 2-R construct. B) Tubulin C-terminus interacts with tau; arrows indicate the C-termini C) Close-

up of β-tubulin with side chains of amino acids that are within interaction distance to 2-R contruct. D) Close-up of α-tubulin and 2-R construct. α-tubulin in green and β-tubulin in blue and 2-R construct is in yellow.

FL-Tau and minimal constructs lead to a MT lattice compression

The addition of tau to dynamic MTs alters the helical lattice parameters of MTs (for a review of lattice parameter definition, refer to Chapter 2 and Figure 2.1). When dynamic MTs are mixed and washed with FL-tau, the lattice of the MTs is compacted with an axial repeat of 80.69 Å. (Table 3.1), distinct from the lattice parameters of the dynamic GDP-MTs with no drugs or MAPs added (81.6 Å). 2-R and 4-R constructs caused a further compaction in the MT lattice (80.15 Å and 80.21 Å respectively) (Table 3.1). The axial repeat has been used as a basis for comparing drug-free MT lattice either bound to GMPCPP (corresponding to a GTP-like state), GDP or GTPγS (Zhang et al. 2015). MTs bound to GMPCPP were shown to have an 'expanded lattice' with a 83.1 Å axial repeat whereas the dynamic, GDP-bound MT has a 'compacted lattice' with an axial repeat of 81.6 Å (Zhang et al. 2015). Our data shows that all of our tau constructs result in further compaction in the MT lattice, beyond the previously reported GTP-bound lattice, with the repeat constructs exhibiting more sever compaction. FL-tau results in a compaction that is similar in magnitude to zampanolide-MTs (Table 2.1B) but none of the tau constructs seem to affect the axial twist. In addition, in the presence of any tau construct, the MT protofilament distribution shifts to 14pfs (87% of the MTs were 14pf with FL-tau, and over 65% were 14pf in the presence of the minimal constructs) as opposed to equal distribution between 13 and 14pf without tau), confirming what has been previously reported (Choi et al. 2009). This finding suggests that tau directly or indirectly affects the lateral interactions between MTs or that it preferentially stabilizes14pf MTs.

Table 3.1 Helical parameters for 14pf MT reconstructions with FL-tau, 2-R construct and 4-R construct added post MT polymerization.

Drug	#of particles	Estimated resolution (Å)	Dimer Rise (Å)	Dimer Twist (°)	Axial Rise (Å)	Axial Twist (°)
FL-tau	21934	4.30	8.64	-25.76	80.68	-0.44
2-R	16447	4.80	8.59	-25.76	80.15	-0.44
4-R	24272	4.30	8.59	-25.76	80.21	-0.44
GDP-MT	N/A	N/A	8.76	-25.76	81.5	-0.46
GMPCPP-MT	N/A	N/A	8.92	-25.80	83.1	-0.34

Despite the similar amount of data (>20,000 particles) that went into the reconstructions of MTs decorated with FL-Tau and MTs decorated with 4-R construct (Table 3.1), and the similar average resolution for the density maps, Fourier shell correlation curves (FSC) show differences in resolution between the two maps (Figure 3.11). This could be due to the quality of

data, which is unlikely because similar protocols and microscope settings were used when obtaining all reconstructions. The other explanation could be that FL-tau is better at stabilizing MTs than 4-R construct. It is possible that elements in the FL-tau that are not present in the 4-R construct are important for ordering the MTs, leading to better behaved samples. To gain insights into the resolution distribution of our reconstructions, we obtained local resolution estimates for MT decorated with FL-tau, 4R- or 2-R construct (Figure 3.12). Local resolution estimates for MTs bounds to any tau construct show that the tau density is lower in resolution than the rest of the MT, and is estimated to be close to 5.5-6Å (Figure 3.12). Surprisingly, the resolution of tubulin in MTs bound to FL-tau is higher than the resolution of tubulin when bound to 4-R construct which further indicates that FL-tau leads to more stable MTs. This finding has implications for future efforts to extend the map resolution. While it is possible to obtain higher resolution maps of tubulin, it is likely that tau would remain at lower resolution than the rest of the map, hindering the identification of amino acids on tau that are essential for MT binding via cryo-EM.

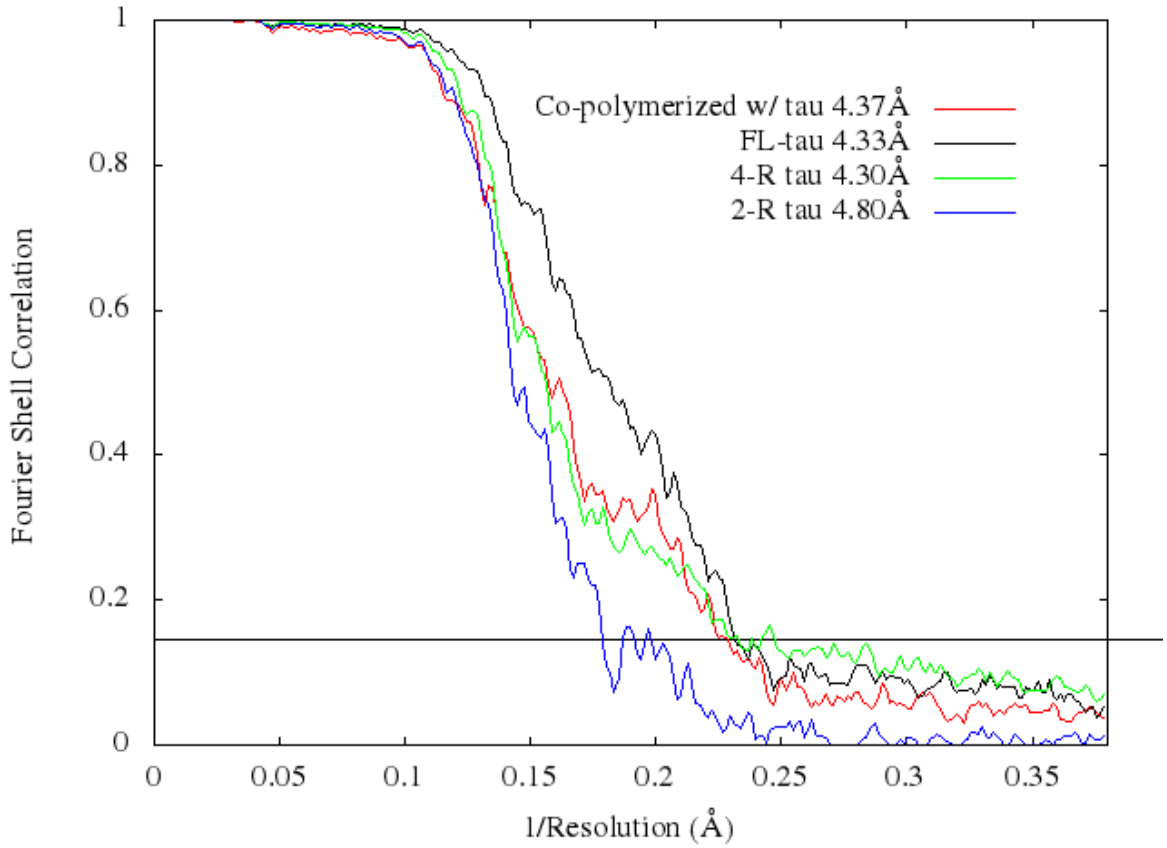

Figure 3.11: Fourier Shell Correlation (FSC) for all MT-tau reconstructions

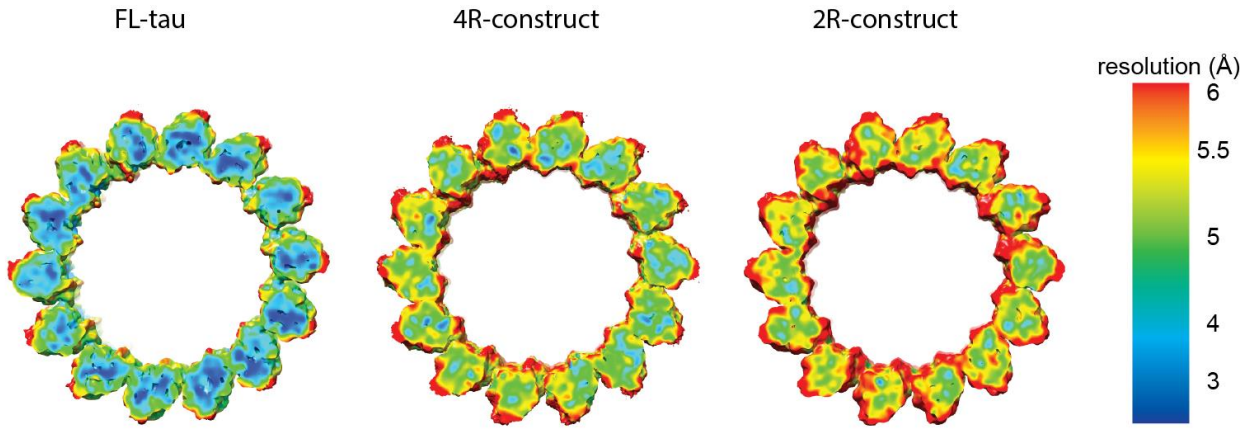

Figure 3:12: Local resolution estimates for MT reconstructions decorated with minimal tau repeats

Discussion

Since its identification as a MAP (Weingarten et al. 1975, Cleveland et al. 1977), the binding location of tau on MTs and its mechanism of action have been controversial. Our data shows that tau binds exclusively on the outside of MTs near the C-terminus and that the binding is longitudinal along MT protofilaments, confirming a previously reported model (Al-Bassam et al 2002). We were able to see extra density corresponding to tau on the surface of MTs; the previously reported models for tau binding were dependent on imaging fiducial markers on tau, NMR or biochemical assays. Furthermore, the reconstructions of FL-tau bound to MTs show that the interaction between FL-tau and MTs happens through extended regions of the tau protein. Tau's ability to bind MTs is attributed to the presence of an imperfect repeat domain (Gustke et al. 1994, Goode and Feinstein 1994) near the C-terminus. The N-terminal domain, also known as the projection domain, has been proposed to function as a spacer between MTs in the axons (Chen at al. 1992). Our data shows that in the absence of the majority of the N-terminus, 2-R and 4-R constructs result in severe MT bundling in contrast to the FL-tau which contains the N-terminus. Furthermore, the absence of density attributed to the N-terminus in our reconstructions for FL-tau suggests that the N-terminus of tau is flexible and untethered to the MT lattice allowing it to act as a spacer between axonal MTs.

The ability of tau to promote tubulin polymerization has been previously reported (Drechsel et al., 1992). Our electron micrographs show that tubulin polymerizes below its critical concertation in the presence of tau confirming what was previously reported. Given tau's ability to bind multiple tubulin dimers, it is conceivable that tau increases the polymerization rate by increasing the local concentration of tubulin, increasing the likelihood of a nucleation event, the rate limiting step of MT polymerization. In vitro, MT assembly occurs in two phases, nucleation and elongation. The kinetic barrier to nucleation inhibits spontaneous and random MT polymerization in the cytoplasm, making nucleation regulation essential for the function and intracellular dynamics of MTs (Desai & Mitchison, 1997). The effects of 2-R and 4-R construct on MT polymerization were comparable to FL-tau, suggesting that the elements of FL-tau needed to alter MT polymerization dynamics are present in the minimal constructs.

Our electron microscopy reconstructions showed that FL-tau, 2-R construct and 4-R construct bind along MT protofilaments near the acidic tubulin C-terminus and result in a slight

increase in the C-terminus structure. The involvement of the negatively charged C-terminus in binding MAPs has been characterized for many MAPs, including MAP2 and motor proteins like dynein (Pashal et al. 1989). The highly acidic and exposed tubulin C-terminus allows electrostatic interactions with positively charged patches of many MAPs. MAP2c for instance, binds MTs via the C-terminus and is known to stabilize MTs by mainly reducing the frequency and duration of catastrophes (Gamblin et al.1996). It is conceivable that tau stabilizes MTs in a similar fashion to MAP2c through interacting with tubulin C-terminus and at least partially neutralizing its charge. It is well know that the phosphorylation of tau results in its dissociation from MTs (Marklund et al. 1996, Horwitz et al. 1997, Chang et al. 2001), which further confirms the role of the electrostatic interactions between tau and the C-terminus for tau binding and function. Surprisingly, the tubulin amino acids we identified to interact with tau are different in α- and β-tubulin, and none of them are among the amino acids that are conserved between the monomers (Figure 3.13). This finding further suggests that tau stabilizes MTs partially through the electrostatic interactions with the C-terminus.

Figure 3.13: **Sequence alignment of H11 and H12 for α- and β-tubulin. Conserved amino acids are highlighted in blue.** Amino acids that interact with tau are boxed. Adapted from Lowe et al, 2001.

The sleeve-like structures observed in the presence of tau are likely to be tubulin dimers that bind to tau decorating the MTs. Since the sleeve-structure was observed extensively in the presence of 2-R construct in contrast to the FL-tau (~65% of the MTs have a sleeve in the presence of 2-R vs ~5% in the presence of FL-tau), it is conceivable that the N-terminus of tau acts as a shield preventing unspecific interaction between the tau decorating axonal MTs and free tubulin dimers. The sleeve structure also suggests that tau is capable of binding free tubulin, in addition to a single tau's ability to bind multiple tubulin dimers (Elbaum-Garfinkle et al. 2014, Li et al. 2015). It is also possible that the sleeve-like structures are more prevalent with the 2R-construct because FL-tau is more efficient than 2-R construct at MT polymerization, leaving fewer free tubulin dimers in solution to form the sleeves in the presence of FL-tau.

Our data shows that MT helical lattice parameters are altered when decorated with tau, with all tested tau constructs yielding a compressed MT lattice and the minimal constructs having a more pronounced effect. The compression observed in the MT lattice could be due to tau binding along individual protofilaments which results in strengthening of the interdimer interactions and a decrease in the axial rise. Other MAPs such as End-binding proteins (EBs), particularly EB3, have been recently shown to modulate structural transitions at MT ends and introduce a "supertwist" in the MT lattice (Zhang et al. 2015). While tau does not alter the supertwist of MTs, it could be modulating MT dynamics by altering the tubulin dimer structure or capturing and stabilizing an intermediate in the GTP-hydrolysis cycle that is more compacted than the GTP-bound state. Interestingly, zampanolide addition to MTs forms stable MTs with a similarly compressed MT lattice (80.79Å). If and how lattice compression beyond the GDP-MT

lattice modulates MT dynamic instability is an interesting question that requires further investigation.

The tubulin double rings that were observed when sub-stoichiometric amounts of tau were added to MTs have been characterized previously as GDP-tubulin rings which form as microtubules depolymerize or from GDP-tubulin as de novo double rings (Nogales at al. 2003). The tubulin double rings are usually observed at low temperatures and high concentrations of magnesium or other divalent cations, and in the absence of GTP (Lobert et al. 1991), conditions that favor MT depolymerization. It is well established that tubulin rings are formed by curled protofilaments, in which the GDP-tubulin bend into a relaxed conformation from the straight form within a MT. FL-tau, might recognize and preferentially bind to the compressed MT lattice of tubulin in the GDP-state. Furthermore, it is possible that different stoichiometric amounts of tau are needed for nucleation and stabilization. A small amount of tau could promote nucleation but not be sufficient to distribute along the length of the resultant MTs to effect stabilization. It seems likely that the sub-stoichiometric amount of tau used in one of our studies was sufficient to facilitate the nucleation of more MTs that it could stabilize. Dynamic MTs formed, but in the absence of sufficient amounts of tau to bind at the stoichiometry needed for MT stability, some MTs depolymerized into the rings that we observed. Higher levels of tau would provide sufficient stability to avoid such depolymerization.

Kinesin binds along the crest of MT protofilaments and has been suggested to compete with tau for binding on MTs (Trinczek et al. 1999). Our data confirms that kinesin competes with FL-tau binding to MTs. This finding is not surprising because kinesin binds to the surface of β-tubulin, and most of the amino acids that interact with tau are present on β-tubulin. In axons, tau is normally associated with most MTs, and the overexpression of tau is known to inhibit kinesin from binding to MTs leading to interference with the plus-end vesicle trafficking (Ebneth et al. 1998). Under our experimental conditions, kinesin had higher affinity to tubulin, since it displaced FL-tau. The relative affinity of kinesin and tau to MTs could be modulated by other factors in the axons.

Despite the valuable insights we obtained on tau binding mode and mechanism for stabilizing MTs, there are many questions to yet be addressed. Identifying the accurate binding stoichiometry and tau's orientation upon binding MTs are essential for understanding the nature of the interaction. We are currently working on producing a 2-R minimal construct with maltose binding protein (MBP) fusion on the N- or C-terminus. Because MBP is a globular protein, we can use it as a marker to deduce the stoichiometry and the polarity of tau on MTs in cryo-EM micrographs. In addition, we are using computational methods to model tau MT interaction. Further experiments to assess the importance of the tubulin acidic C-terminus in tau binding would be valuable in addition to understanding how MT lattice compression could alter its dynamics.

Chapter Four: Conclusions and Outlook

The discovery of MT dynamic instability was essential for understanding how MTs can reassemble into diverse structures providing dividing cells the plasticity they need during development. Dynamic instability has been known for over thirty years to be driven by GTP hydrolysis (Mitchison & Krischner, 1984), but it was not until recently that we gained mechanistic and structural insights of the process (Alushin et al. 2014, Zhang et al. 2015). The transition from a GTP-bound state to a GDP-bound state leads to a MT lattice compaction around the E-site at longitudinal interfaces in addition to a movement of the intermediate domain and H7 helix of α-tubulin (Alushin et al. 2014). The changes around the E-site upon nucleotide hydrolysis lead to global lattice rearrangement of the MT and generate strain in the lattice (Zhang et al. 2015). A dynamic MT, which is constituted mostly of tubulin in the GDP-bound state, would be strained and the MT would have a compacted lattice. In the presence of a GTP-cap, the strained lattice is "locked" in that state, and upon the hydrolysis of the GTP-cap, the strain causes the MT to depolymerize (Alushin et al 2014, Zhang et al. 2015). MTs in the GTP-bound state can be formed by using a non-hydrolysable GTP analog such as GMPCPP. These MTs have extended lattices and have a "straight conformation". It has been suggested that Taxol and other anticancer-drugs stabilize MTs by allosterically inducing a GMPCPP-like extended lattice. Our drug studies in Chapter 2 confirm that Taxol-bound MTs have an extended lattice structure mimicking the GMPCPP state (Elizabeth Kellogg, manuscript in preparation). However, while zampanolide does affect the tubulin conformation and MT lattice, the MT lattice is distinct from that induced by Taxol; in fact the MT lattice is compacted beyond a GDP-bound lattice, suggesting that dynamic instability is modulated differently by different drugs.

It was long hypothesized that MTs could be stabilized in vivo upon interacting with cellular structures (Krishner & Mitchison, 1986) or soluble entities (Karsenti, 1991; Hyman & Karsenti, 1996). The discovery of kinetochore-MT interactions (Hayden et al., 1990) was the initial confirmation of the hypothesis. Many proteins and small molecules have been shown to modulate MT dynamics since then. Some of the MAPs, such as EB3 (Zhang et al. 2015) and Doublecortin (DCX) (Fourniol et al. 2010), have been shown to associate with MTs via sensing the different curvature of the MT lattice. Motor domains, such as kinesins and dyneins, use ATP hydrolysis cycle to modulate their affinity to MT binding (Gennerich & Vale, 2009). Most MAPs however, interact with MTs via the acidic tubulin C-terminus which extends from the surface of MTs. The C-terminus is the most common site for post-translational modifications (Janke 2014), and it plays an essential role in MAP binding.

The effects of the C-terminus on MT dynamics are intriguing. Partial proteolysis of the tubulin C-terminus by subtilisin leads to MT polymerization under conditions that prohibit MT assembly of undigested tubulin. Furthermore, the cleaved tubulin polymerizes at concentrations below the normal tubulin critical concentration (Serrano et al. 1984). The partial cleavage of the tubulin C-terminus affects MT dynamics in a manner comparable to adding a structural MAP, particularly MAP2 (Serrano et al. 1984) and tau. Furthermore, tubulin with subtilisin-cleaved C-terminus assembles into protofilament bundles and open tubule structures (Serrano et al. 1984) which indicates that the removal of the acidic C-terminus facilitates protofilament interactions. The repulsion of the highly charged C-terminus of adjacent tubulin dimers could be a destabilizing force in a MT lattice, thus, the removal of the charged amino acids via subtilisin cleavage could enhance protofilament interactions within a MT lattice. It is conceivable that MAPs which bind to MT via the C-terminus stabilize MTs and alter their dynamics merely by

shielding the negative charge of the C-terminus, eliminating the destabilizing repulsion of the C-terminus. Tau seems to bind and stabilize MTs by sequestering the C-terminus in addition to tethering the tubulin subunits together along a protofilament, leading to lattice stability. Tau also alters the helical parameters of MTs, leading to a compaction in the MT lattice beyond that of the GDP-bound state. Collectively, my work suggests that the extended MT lattice is not the only stable lattice. I speculate that the GDP-bound MT lattice is the unstable conformation of the lattice. It is possible that compaction beyond the GDP-bound lattice results in MT stability similar to the extended lattice. This state could be an intermediate state in the nucleotide hydrolysis cycle. In fact, MTs bound to GTPγS, which mimics the GDP-Pi state, have a compacted lattice (81.0Å) in comparison to the GDP-bound state and GTPγS-bound MTs are dynamically stable (Rui Zhang, personal communication). While my experiments and findings support such a model, further experiments are required to validate this hypothesis.

Many of the MAPs that have been recently identified belong to a class of proteins known as intrinsically disordered proteins (IDPs). IDPs have gained recognition in the last decade given that many eukaryotic proteins or regions of functional proteins are IDPs under native conditions (Babu et al 2011). IDPs have been associated with diseases and their disordered nature is crucial for their functions in the cell (Tompa 2012). The lack of a unique 3D structure allows these proteins to have conformational flexibility and the ability to interact with numerous other proteins due to a larger interaction surface area (Babu 2011). Some of the IDPs are known to fold upon binding, and despite their disordered nature, IDPs bind to their partners with high specificity and low affinity enabling them to modulate regulatory events in space and time (Write and Dyson, 2009). Many MAPs are known to belong to the IDP family, most notably tau and MAP2.

Recently, more MAPs that are IDPs have been discovered including MDM1 (Van de Mark, 2015), Tobacco Mosaic Virus movement protein (TMV-MP) (Heinlein at al. 1995), MAP6 (Pabio et al 1984), Fam154 A and Fam154 B proteins (Irene Onyeneho and Tim Stearns, unpublished data). Throughout my Ph.D, I studied several other MAPs that are also known to be IDPs via cryo-EM, including TMV-MP, MDM1, Fam154 A and Fam145 B. MDM1, Fam154 A and Fam154 B have been shown to stabilize MTs and modulate their dynamics. All of these proteins consist of multiple conserved repeat domains that are known to bind and stabilize MTs. I have been able to show that MDM1 and TMV-MP associate with MTs in cryo-EM micrographs (Figure 4.1). However, further data processing and analysis did not yield unambiguous extra densities corresponding to these proteins. This could be because MDM1 and TMV-MP bind mostly through the flexible tubulin C-terminus and remain largely unstructured upon binding rendering the currently used image data processing algorithm unable to detect a footprint for these proteins. It is possible that all IDP MAPs interact with MTs via the highly acidic tubulin C-terminus shielding its negative charge and stabilizing MTs through reduction of electrostatic repulsion. The effects of cleaving the tubulin C-terminus via subtilisin seems to recapitulate the effects of these IDP MAPs on MT dynamics and stability, further suggesting that these MAPs stabilize MTs via interacting with the C-terminus. However, cleaving the C-terminus with subtilisin does not abolish binding. We and others have done numerous assays that indicate binding of these proteins to subtilisin-cleaved tubulin. The Tau density on MTs in our reconstructions in Chapter 3, albeit weak, is the most we have seen for any of the IDP MAPs. Electron microscopy, although powerful, might not be the best suited tool for studying IDPs that remain extended upon binding to their partners.

Collectively, the mechanism by which MT dynamics are modulated is not universal. While we have a much better understanding of how some effectors regulate MT dynamic instability, we are far from understanding the full mechanistic details of how others induce polymerization and stability. For IDPs, we need to rely heavily on computational modeling and point mutations to understand the nature of the interaction.

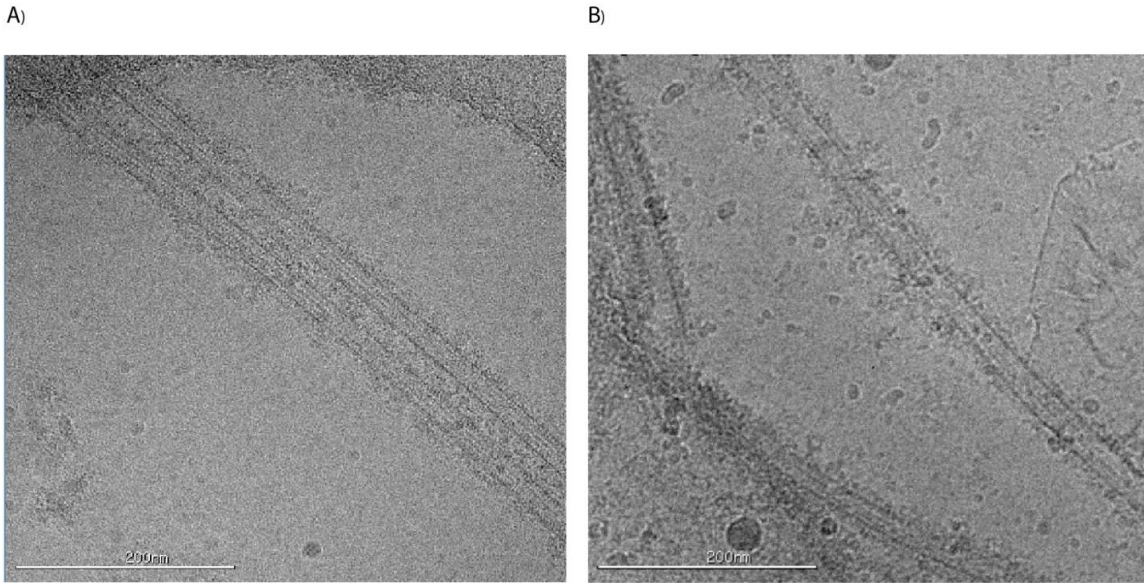

Figure 4.1: **Micrographs of intrinsically disordered MAPs interacting with MTs**. A) MDM1 decorating MTs B) TMV-MP decorating MTs.

Chapter Five: References

Aizawa, H., Emori, Y., Murofushi, H., Kawasaki, H., Saka, H., Suzuki, K. (1990). "Molecular cloning of a ubiquitously distributed microtubule associated protein with Mr 190,000." J Biol Chem, **265**(23): 13849–13855.

Akhmanova, A., Steinmetz, M. (2008). "Tracking the ends: a dynamic protein network controls the fate of microtubule tips." Nat. Rev. Mol. Cell Biol., **9**: 309-322.

Al-Bassam, J., Ozer, R., Safer, D., Halpain, S., Milligan, R.A. (2002) "MAP2 and tau bind longitudinally along the outer ridges of microtubule protofilaments". J. Cell Biol., **157** (7): 1187-1196.

Alushin, G.M., Lander, G.C., Kellogg, E.H., Zhang, R, Baker, D., Nogales, E. (2014). "High-resolution microtubule structures reveal the structural transitions in αβ-tubulin upon GTP hydrolysis." Cell, **157**(5): 1117-1129.

Amos, L.A. (2004). "Microtubule structure and its stabilization." Org. Biomol. Chem., **2**: 2153-2160

Amos, L.A., Lowe, J. (1999). "How Taxol stabilises microtubule structure." Chem Biol, **6**(3): R65-69.

Amos, L.A., Klug, A. (1974). "Arrangement of subunits in flagellar microtubules." J. Cell Sci., **14:** 523-549.

Andreu, J. M., Ghosh, A. K., Giannakakou, P., Hamel, E. (2002). "The microtubule stabilizing agent laulimalide does not bind in the taxoid site, kills cells resistant to paclitaxel and epothilones, and may not require its epoxide moiety for activity." Biochem., **41**: 9109-15.

Arnal, I., Wade R.H. (1995). "How does Taxol stabilize microtubules?" Curr. Biol., **5**(8): 900-908.

Babu, M. M., Van der Lee, R., Sanches de Groot, N., Gsponder, J. (2011). "Intrinsically disordered proteins: regulation and disease." Curr. Opin. Struct. Biol., **21**(3): 432-440.

Bai, X. C., Fernandez, I. S., McMullan, G., Scheres, S. H. (2013). "Ribosome structures to near-atomic resolution from thirty thousand cryo-EM particles." Elife, **2**: e00461.

Best, H. A., Matthews, J. H., Heathcott, R. W., Hanna, R., Leahy, D. C., Coorey, N. V, Bellows, D. S., Atkinson, P. H., Miller, J. H. (2013). "Laulimalide and Peloruside A inhibit mitosis of Saccharomyces cerevisiae by preventing microtubule depolymerisation-dependent steps in chromosome separation and nuclear positioning." Mol. Biosyst., **9**(11): 2842-2852.

Biernat, J., Gustke, N., Drewes, G., Mandelkow, E. (1993). “Phosphorylation of Ser^{262} strongly reduces binding of tau to microtubules: Distinction between PHF-like immunoreactivity and microtubule binding.” Neuron, **11**(1): 153-163.

Buey, R.M. E. Calvo, I. Barasoain, O. Pineda, M.C. Edler, R. Matesanz, G. Cerezo, C.D. Vanderwal, B.W Day, E.J Sorensen (2007). “Cyclostreptin binds covalently to microtubule pores and luminal taxoid binding sites” Nat. Chem. Biolo., **3**: 117-125

Boder, G. B., Paul, D. C., Williams, D.C. (1983). “Chlorpromazine inhibits mitosis of mammalian cells.” Eur. J. Cell Biol., **31**: 349-353.

Bonnet, C., Boucher, D., Lazereg, S., Pedrotti, B., Islam, K., Denoulet, P., Larcher, J. C. (2001). “Differential binding regulation of microtubule-associated proteins MAP1A, MAP1B, and MAP2 by tubulin polyglutamylation.” J. Biol. Chem., **276**(16): 12839-48.

Brandt, R., Lee, G. (1993). “Functional Organization of Microtubule-associated Protein Tau: Identification of regions which affect microtubule growth nucleation and bundling formation in vitro.” J. Cell Biol., **268**(5): 3414-3419.

Cassimeris, L., Spittle, C. (2001). “Regulation of microtubule-associated proteins.” Int. Rev. Cytol, **210**: 163-226.

Chan, A., Andreae, P. M., Northcote, P. T., Miller, J. H. (2011). "Peloruside A inhibits microtubule dynamics in a breast cancer cell line MCF7." Invest. New Drugs, **29**(4): 615-626.

Chang, W., Gruber, D., Chari, S., Kitazawa, H., Hamazumi, Y., Hisanaga, S., Bulinski, J. C. (2001). “Phosphorylation of MAP4 affects microtubule properties and cell cycle progression.” J. Cell Sci., **114**: 2879-87.

Chen, J., Kanai, Y., Cowan, N. J., Hirokawa, N. (1992). “Projection domains of MAP2 and tau determine spacings between microtubules in dendrits and axons.” Nature **360**: 674-7.

Choi, M. C., Raviv, U., Miller, H. P., Gaylord, M. R., Kiris, E., Ventimiglia, D., Needleman, D.J., Kim, M. W., Wilson, L., Feinstein, S. C., Safinya, C. R. (2009). “Human microtubule associated-protein tau regulates the number of protofilaments in microtubules: a synchrotron xray scattering study.” Biophys. J, **97**: 519-27.

Chretien, D., Metoz, F., Verde, F., Karsenti, E., Wade, R. H. (1992). "Lattice defects in microtubules: protofilament numbers vary within individual microtubules." J. Cell Biol., **117**(5): 1031-1040.

Cleveland, D. W., Hwo, S. Y., Kirschner, M. W. (1977). “Physical and chemical properties of purified tau factor and the role of tau in microtubule assembly.” J. Mol. Biol., **116**: 227-47.

Cormier A, Knossow M, Wang C, Gigant B. (2010). “The binding of vinca domain agents to tubulin: structural and biochemical studies”. Methods Cell Biol **95**: 373–90.

Desai, A., Mitchison, T. (1997). “Microtubule polymerization and dynamics.” Annu. Rev. Cell Dev. Biol., **13**: 83-117.

Diaz, J. F., Valpuesta, J. M., Chacon, P., Diakun, G., Andreu, J. M. (1998). "Changes in microtubule protofilament number induced by Taxol binding to an easily accessible site. Internal microtubule dynamics." J. Biol. Chem, **273**(50): 33803-33810.

Díaz-Valencia, J. D., Morelli, M. M., Bailey, M., Zhang, D., Sharp, D. J., Ross, J. L. (2011). “Drosophila katanin-60 depolymerizes and severs at microtubule defects.” Biophysical Journal **100**(10): 2440–9.

DiMaio, F., Song, Y., Li, X., Brunner, M. J., Xu, C., Conticello, V., Egelman, E., Marlovits, T. C., Cheng, Y., Baker, D. (2015). "Atomic-accuracy models from 4.5-A cryo-electron microscopy data with density-guided iterative local refinement." Nat. Methods **12**(4): 361-365.

Ding, F., Jennings, M. P. (2008). "Total synthesis of (-)-dactylolide and formal synthesis of (-)-Zampanolide via target oriented beta-C-glycoside formation." J. Org. Chem.,**73** (15): 5965-76.

Downing, K. H. (2000). “Structural basis for the interaction of tubulin with proteins and drugs that affect microtubule dynamics.” Annu. Rev. Cell. Dev. Biol. **16**(1): 89-111.

Drechsel, D. N., Hyman, A. A., Cobb, M. H., Kirschner, M. W. (1992). “Modulation of the dynamic instability of tubulin assembly by the microtubule-associated protein tau.” Mol. Biol. Cell, **3**(10): 1141-54.

Drubin D. G, Kirschner, M. W. (1986). “Tau protein function in living cells.” J. Cell Biol., **103**(6): 2739–2746.

Dumontet, C. and M.A. Jordan (2010). “Microtubule-binding agents: a dynamic field of cancer therapeutics”. Nat. Red. Drug. Discov., **9**: 790-803

Dumont S., Mitchison T. J. (2009). “Force and length in the mitotic spindle.” Curr. Biol,**19**(17): 749-61.

Dye, R. B., Fink, S. P., Williams Jr., R. C. (1993). "Taxol-induced flexibility of microtubules and its reversal by MAP-2 and Tau." J. Biol. Chem **268**(10): 6847-6850.

Ebneth, A., Godemann, R., Stamer, K., Illenberger, S., Trinczek, B., Mandelkow, E. (1998). “Overexpression of tau protein inhibits kinesin-dependent trafficking of vesicles, mitochondria, and endoplasmic reticulum: implications for Alzheimer's disease.” J. Cell Biol.,**143**: 777-94.

Elbaum-Garfinkle, S., Cobb, G., Compton, J., Li, X., Rhoades, E. (2014). “Tau mutants bind tubulin heterodimers with enhanced affinity.” Proc. Natl. Acad. Sci., **111**(17): 6311-6316.

Elie-Caille, C., Severin, F., Helenius, V, Howard, J., Muller, D. J., Hyman, A. A. (2007). "Straight GDP-tubulin protofilaments form in the presence of Taxol." Curr. Biol. **17**(20): 1765-1770.

Eliezer, D., Barré, P., Kobaslija, M., Chan, D., Li, X., Heend, L. (2005). "Residual structure in the repeat domain of tau: echoes of microtubule binding and paired helical filament formation." Biochemistry **44**: 1026-36.

Erickson, H. P. (1998). "Atomic structures of tubulin and FtsZ". Trends Cell Biol.,**8**: 133–7.

Field, J., Pera, B., Calvo, E., Canales, A, Zurwerra, D., Triqili, C., Rodriquez-Salarichs, J., Matesanz, R., Kanakkanthara, A., Wakefield, J., Singh, J., Jimenez-Barbero, J., Northcote, P., Miller, J. H., Antonio Lopez, J., Hamel, E., Barasoain, I., Altmann, K. H., Dıaz, J. F. (2012). "Zampanolide, a Potent New Microtubule-Stabilizing Agent, Covalently Reacts with the Taxane Luminal Site in Tubulin a,b-Heterodimers and Microtubules." J. Chem. Bio. **19** (6): 686-98.

Field, J., Singh, A. J., Kanakkanthara, A., Halafihi, T., Northcote, P. T., Miller, J.H. (2009). "Microtubule-Stabilizing Activity of zampanolide, a Potent Macrolide Isolated from the Tongan MarineSponge Cacospongia mycofijiensis." J. Med. Chem **52**(22): 7328-32

Fourniol, F.J., C.V. Sindelar, B. Amigues, D. K. Clare, G. Thomas, M. Perderiset, F. Francis. A. Houdusse, C.A Moores.(2010). "Template-free 13-protofilament microtubule-MAP assembly visualization at 9A resolution." J. Cell Biol. **191**: 463-470.

Gaitanos, T. N., R. M. Buey, J. F. Diaz, P. T. Northcote, P. Teesdale-Spittle, J. M. Andreu and J. H. Miller (2004). "Peloruside A does not bind to the taxoid site on beta-tubulin and retains its activity in multidrug-resistant cell lines." Cancer Res. **64**(15): 5063-5067.

Gamblin TC, K. Nachmanoff, S. Halpain, R.C.Williams Jr (1996). "Recombinant microtubule-associated protein 2c reduces the dynamic instability of individual microtubules." Biochemistry **35**: 12576-12586.

Garcia, M. L., and Cleveland, D. V. (2001). "Going new places using an old MAP: tau, microtubules and human neurodegenerative disease." Curr. Opin. Cell Biol. **13**: 41–48.

Gennerich, A., R.D Vale (2009). "Walking the walk:how kinesin and dynein coordinate their steps". Curr. Opin. Cell Biol. **21**: 59-67.

Gerth, K., N. Bedorf, G. Hofle, H. Irschik and H. Reichenbach (1996). "Epothilons A and B: antifungal and cytotoxic compounds from Sorangium cellulosum (Myxobacteria). Production, physico-chemical and biological properties." J. Antibiot (Tokyo) **49**(6): 560-563.

Goedert, M, Spillantini M. G., Jakes R., Rutherford D., Crowther R. A. (1989). "Multiple isoforms of human microtubule-associated protein tau: Sequences and localization in neurofibrillary tangles of Alzheimer's disease." Neuron, **3**(4):519–526.

Goedert, M., Jakes, R. (1990). “Expression of separate isoforms of human tau protein: correlation with the tau pattern in brain and effects on tubulin polymerization.” The EMBO Journal, **9**(13): 4225-4230.

Goedert, M., M. G. Spillantini, N. J. Carins, R. A. Crowther (1992). “Tau proteins of Alzheimer paired helical filaments: abnormal phosphorylation of all six brain isoforms.” Neuron, **8**(1):159-168.

Goedert, M., Wischik, C. M., Crowther, R. A., Walker, J. E., Klug, A. (1998). “Cloning and sequencing of the cDNA encoding core of the paired helical filament of Alzheimer’s disease.” Proc. Natl. Acad. Sci., **85**(11): 4051–4055.

Goode, B. L., Feinstein, S. C. (1994). “Identification of a novel microtubule binding and assembly domain in the developmentally regulated inter-repeat region of tau.” J. Cell Biol., **124**: 769-82.

Goode, B., P. Denis, D. Panda, M. Radeke, H. Miller, L. Wilson, S. Feinstein (1997). “Functional Interactions between the Proline-rich and Repeat Regions of Tau Enhance Microtubule Binding and Assembly.” Mol. Biol. Cell., **8**: 353-365.

Gustke N., Trinczek B., Biernat J., Mandelkow E. M., Mandelkow E. (1994). “Domains of tau protein and interactions with microtubules.” Biochemistry, **33**(32): 9511–9522.

Hamel, E., B. W. Day, J. H. Miller, M. K. Jung, P. T. Northcote, A. K. Ghosh, D. P. Curran, M. Cushman, K. C. Nicolaou, I. Paterson and E. J. Sorensen (2006). "Synergistic effects of Peloruside A and laulimalide with taxoid site drugs, but not with each other, on tubulin assembly." Mol. Pharmacol, **70**(5): 1555-1564.

Harindranat, K. R. V. Hofelea, J. Biernatb, S. Kumarb, K. Tepperb, H. Urlauba, E. Mandelkowb, M. Zweckstettera (2015). “Tau stabilizes microtubules by binding at the interface between tubulin heterodimers” Proc. Natl. Acad. Sci.,**112**(24): 7501-7506.

Hawkins, T. L., D. Sept, B. Mogessie, A. Straube and J. L. Ross (2013). "Mechanical properties of doubly stabilized microtubule filaments." Biophys. J,**104**(7): 1517-1528.

Hayden, J. H., Bowser, S. S., Rieder, C. L. (1990). “Kinetochores capture astral microtubules during chromosome attachment to the mitotic spindle: direct visualization in live newt lung cells.” J. Cell Biol., **111**: 1039-1045.

Hebert L. E, J. Weuve, P. A. Scherr, D. L. Evans (2013). “Alzheimer disease in the United States (2010–2050) estimated using the 2010 census.” *Neurology*,**80**: 1778-83.

Heymann, J. B., Cardone G., Winkler D. C., Steven A. C. (2008) “Computational resources for cryo-electron tomography in Bsoft.” J. Struct. Biol., **161**(3), 232 – 242.

Hirokawa, N. (1998). “Kinesin and Dynein Superfamily Proteins and the Mechanism of Organelle Transport” Science, **279:** 519-526.

Hood, K. A., L. M. West, B. Rouwe, P. T. Northcote, M. V. Berridge, S. J. Wakefield and J. H. Miller (2002). "Peloruside A, a novel antimitotic agent with paclitaxel-like microtubule-stabilizing activity." Cancer Res., **62**(12): 3356-3360.

Horwitz, G. A. Orr (2006). "Insights into the mechanism of microtubule stabilization by Taxol." Proc. Natl. Acad. Sci., **103**(27): 10166-10173.

Horwitz, S. B., H. J. Shen, L. He, P. Dittmar, R. Neef, J. Chen, U. K. Schubart (1997). "The microtubule-destabilizing activity of metablastin (p19) is controlled by phosphorylation." J. Biol. Chem, **272**: 8129-32.

Hutton, M., C. L. Lendon, P. Rizzu, M. Baker, S. Froelich, H. Houlden, J. Hackett (1998). "Association of missense and 5′-splice-site mutations in tau with the inherited dementia FTDP-17." Nature, **393**(6686): 702-705.

Huzil, J. T., J. K. Chik, G. W. Slysz, H. Freedman, J. Tuszynski, R. E. Taylor, D. L. Sackett (2008). "A unique mode of microtubule stabilization induced by peloruside A." J. Mol. Biol., **378**(5): 1016-30.

Hyman, A. A., Karsenti, E. (1996). "Morphogenetic properties of microtubules and mitotic spindle assembly." Cell, **84**: 401-410.

Janke C. (2014). "The tubulin code: molecular components, readout mechanisms and functions." J. Cell Biol. **206**: 461-472.

Jimenez-Barbero, J., F. Amat-Guerri, J. P. Snyder (2002). "The solid state, solution and tubulin-bound conformations of agents that promote microtubule stabilization." Curr. Med. Chem. Anti-Canc. Agents, **2**: 91-122.

Jordan, M. A., Wilson, L. (1998). "Microtubules and actin filaments: dynamic targets for cancer chemotherapy." Curr. Opin. Cell Biol., **10**: 123–130 (1998).

Jordan, M. A. (2002). "Mechanism of action of antitumor drugs that interact with microtubules and tubulin." Curr. Med. Chem. Anti-Canc. Agents, **2:**1–17.

Jordan, M., Wilson, L. (2004). "Microtubules as a target for anticancer drugs " Nat. Rev. Cancer, **4**: 353-265.

Kar, S., J. Fan, M. J. Smith, M. Goedert, L. A. Amos (2003). "Repeat motifs of tau bind to the insides of microtubules in the absence of Taxol." The EMBO, **22**: 70-77

Karsenti, E. (1991). "Mitotic spindle morphogenesis in animal cells." Semin. Cell Biol., **2**: 251-260.

Kavallaris, M. (2010). "Microtubules and resistance to tubulin-binding agents." Nature Reviews Cancer, **10**(3): 194-204.

Khrapunovich-Baine, M., V. Menon, C. P. Yang, P. T. Northcote, J. H. Miller, R. H. Angeletti, A. Fiser, S. B. Horwitz and H. Xiao (2011). "Hallmarks of molecular action of microtubule stabilizing agents: effects of epothilone B, ixabepilone, Peloruside A, and laulimalide on microtubule conformation." J. Biol. Chem., **286**(13): 11765-11778.

Kingston DG. (2008). "Tubulin-interactive natural products as anticancer agents." J. Nat. Prod. **72**(3): 507-15.

Kingstone, D. G., S. Bane, J. P. Synder (2005). "The taxol pharmacophore and the T-taxol bridging principal." Cell Cycle, **4**(2): 278-288.

Hodge, M., Q. H. Chen, S. Bane, S. Sharma, M. Loew, A. Banerjee, D. G. Kingston (2009). "Synthesis and bioactivity of a side chain bridge paclitaxel: A test of the T-Taxol conformation." Bioorg. Med. Chem. Lett.,**19** (10): 2884-2887.

Kirschner, M., Mitchison, T. (1986). "Beyond self-assembly: from microtubules to morphogenesis." Cell **45**: 329-342.

Kosik K. S., Orecchio L. D., Bakalis S., Neve R. L. (1989). "Developmentally regulated expression of specific tau sequences." Neuron, **2**(4): 1389–1397.

Kreis, T., and Vale, R. (1999). "Guidebook to the cytoskeleton and motor proteins, 2nd " (Oxford University Press).

Kueh H. Y., Mitchison T. J. (2009). "Structural plasticity in actin and tubulin polymer dynamics." Science,**325**: 960–963.

Larsen E. M.,Wilson, M. R., Zajicek J., Taylor, E.A. (2013). "Conformational Preferences of ZampanolideZampanolide and Dactylolide." Organic Letters,**15** (20): 5246–5249.

Lee, V. M., Balin, B. J., Otvos Jr., L., Trojanowski, J. Q. (1991). "A68: a major subunit of paired helical filaments and derivatized forms of normal Tau." Science, **251**: 675-8.

Leroux, P., R. Fritz, D. Debieu, C. Albertini, C. Lanen, J. Bach (2002). "Mechanisms of resistance to fungicides in field strains of Botrytis cinerea." Pest Manag. Sci., **58**: 876–88.

Li, H., J. Culver, Rhoades, E. (2015). "Tau Binds to Multiple Tubulin Dimers with Helical Structure." J Am Chem Soc. **137**(29): 9218:9221.

Li, J., A. L. Risinger and S. L. Mooberry (2014). "Taccalonolide microtubule stabilizers." Bioorg. Med. Chem., **22**(18): 5091-5096.

Liu, Z., P. Xu, T. Wu and W. Zeng (2014). "Microtubule-targeting anticancer agents from marine natural substance." Anticancer Agents Med. Chem., **14**(3): 409-417.

Lobert S., J. J. Correia (1991). “Studies of crystallization conditions for native and subtilisin-cleaved pig brain tubulin.” Arch Biochem. Biophy., **290**: 93-102.

Lowe, J., H. Li, K. H. Downing and E. Nogales (2001). "Refined structure of alpha beta-tubulin at 3.5 A resolution." J. Mol. Biol., **313**(5): 1045-1057.

Lowe, J., K. H. Downing, E. Nogales (2001). “Refined Structure of ab-Tubulin at 3.5 A Resolution.” J. Mol. Biol., **313**: 1045-1057.

Lyumkis, D., A. F. Brilot, D. L. Theobald and N. Grigorieff (2013). "Likelihood-based classification of cryo-EM images using FREALIGN." J. Struct. Biol., **183**(3): 377-388.

Manfredi, J. J., S. B. Horwitz (1984). "Taxol: an antimitotic agent with a new mechanism of action." Pharmacol. Ther., **25**(1): 83-125.

Marco D. Mukrasch, Bergen, M., Biernat, J., Fischer, D., Griesinger, C., Mandelkow, E., Zweckstetter, M. (2007). “The “Jaws” of the Tau-Microtubule Interaction.” J. Biol. Chem. **282**(16): 12230–12239.

Marklund, U., Larsson, N., Gradin, H. M., Brattsand, G., Gullberg, M. (1996). “Oncoprotein 18is a phosphorylation-responsive regulator of microtubule dynamics.” EMBO J., **15**(19): 5290-5298.

Matesanz, R., J. Rodriguez-Salarichs, B. Pera, A. Canales, J. M. Andreu, J. Jimenez-Barbero, W. Bras, A. Nogales, W. S. Fang, J. F. Diaz (2011). "Modulation of microtubule interprotofilament interactions by modified taxanes." Biophys J, **101**(12): 2970-2980.

McIntosh, J. R., M. K. Morphew, P. M. Grissom, S. P. Gilbert, A. Hoenger. (2009). “Lattice structure of cytoplasmic microtubules in a cultured Mammalian cell.” J. Mol. Biol., **394**: 177-182.

Mitchison, T. J., and Kirschner, M. (1984). “Dynamic instability of microtubule growth.” Nature **312**: 237-242.

Mitchison, T. J. (1993). “Localization of an exchangeable GTP binding site at the plus end of microtubules.” Science, **261**: 1044-1047.

Mooberry, S. L., G. Tien, A. H. Hernandez, A. Plubrukarn and B. S. Davidson (1999). "Laulimalide and isolaulimalide, new paclitaxel-like microtubule-stabilizing agents." Cancer Res. **59**(3): 653-660.

Mukherjee A, C. Saez, J. Lutkenhaus (2001). “Assembly of an FtsZ mutant deficient in GTPase activity has implications for FtsZ assembly and the role of the Z ring in cell division”. J Bacteriol **183**: 7190–7.

Nettles, J. H., H. Li, B. Cornett, J. M. Krahn, J. P. Snyder and K. H. Downing (2004). "The binding mode of epothilone A on alpha,beta-tubulin by electron crystallography." Science **305**(5685): 866-869.

Nogales E., K. H. Downing, L. A. Amos, J. Lowe (1998). “Tubulin and FtsZ form a distinct family of GTPases.” Nat. Struct. Biol., **5**: 451–458.

Nogales, E., H. Wang, H. Niederstrasser (2003). “Tubulin rings: which way do they curve?” Curr. Opin. Struct. Biol., **13**: 256–261

Nogales, E., M. Whittaker, R. A. Milligan and K. H. Downing (1999). "High-resolution model of the microtubule." Cell, **96**(1): 79-88.

Nogales, E., S. G. Wolf and K. H. Downing (1998). "Structure of the alpha beta tubulin dimer by electron crystallography." Nature, **391**(6663): 199-203.

Ojima, I., K. Kumar, D. Awasthi and J. G. Vineberg (2014). "Drug discovery targeting cell division proteins, microtubules and FtsZ." Bioorg. Med. Chem., **22**(18): 5060-5077.

Pashal, P. B., R. A. Obar., R.B. Vallee (1989). “Interaction of brain ctyoplamic dynine and MAP2 with common sequence at the C terminus of tubulin.” Nature, **342**: 569-572

Poulain FE, Sobel A. (2010). “The microtubule network and neuronal morphogenesis: Dynamic and coordinated orchestration through multiple players.” Mol. Cell Neurosci., 43(1): 15-32

Prota, A. E., K. Bargsten, D. Zurwerra, J. J. Field, J. F. Diaz, K. H. Altmann and M. O. Steinmetz (2013). "Molecular mechanism of action of microtubule-stabilizing anticancer agents." Science, **339**(6119): 587-590.

Prota, A. E., K. Bargsten, P. T. Northcote, M. Marsh, K. H. Altmann, J. H. Miller, J. F. Diaz, M. O. Steinmetz (2014). "Structural basis of microtubule stabilization by laulimalide and Peloruside A." Angew Chem. Int. Ed. Engl. **53**(6): 1621-1625.

Prota, A. E., Bargsten, K., Diaz, F. J., Marsh, M., Cuevas, C., Liniger, Neuhaus, C., Andreu, J. M., Heinz-Altmann, K., Steinmetz M. (2014). “A new tubulin-binding site and pharmacophore for microtubule-destabilizing anticancer drugs.” Proc. Natl. Acad. Sci., **111**(38): 13817–13821.

Pryor, D. E., O'Brate, A., Bilcer, G., Díaz, J. F., Wang, Y., Wang, Y., Kabaki, M., Jung, M. K., Rai S. S., Wolff J. (1996). “Localization of the vinblastine-binding site on beta-tubulin.” J. Biol. Chem., **27**1:14707–11.

Risinger A. L., Giles F. J., Mooberry S. L. (2009) “Microtubule dynamics as a target in oncology.” Cancer Treat Rev., **35**: 255–61.

Rohou, A. and N. Grigorieff (2014). "Frealix: model-based refinement of helical filament structures from electron micrographs." J. Struct. Biol., **186**(2): 234-244.

Rohou, A. and N. Grigorieff (2015). "CTFFIND4: Fast and accurate defocus estimation from electron micrographs." J. Struct. Biol., **192**(2): 216-21

Sakamoto, T., Uezu, A., Kawauchi, S., Kuramoto, T., Makino, K., Umeda, K., Nakanishi, H. (2008). “Mass spectrometric analysis of microtubule co-sedimented proteins from rat brain.” Genes Cells, **13**(4) :295-312.

Scheffers D. J., J. G. de Wit, T. den Blaauwen, A. J. Driessen (2000). “GTP hydrolysis of cell division protein FtsZ: evidence that the active site is formed by the association of monomers.” Biochemistry, **41**: 521–9.

Scheres, S. H. (2014). "Beam-induced motion correction for sub-megadalton cryo-EM particles." Elife **3**: e03665.

Schiff, P. B., J. Fant and S. B. Horwitz (1979). "Promotion of microtubule assembly in vitro by Taxol." Nature, **277**(5698): 665-667.

Schriemer, D. C. (2008). “A unique mode of microtubule stabilization induced by Peloruside A.” J. Mol. Biol., **378**(5): 1016-30.

Schweers, O., Schönbrunn-Hanebeck, E., Marx, A., Mandelkow, E. (1994). “Structural studies of tau protein and Alzheimer paired helical filaments show no evidence for beta-structure.” J. Biol. Chem., **269**: 24290-24297.

Serrano, L. Garcini, E., Hernandez, M. Avila, J. (1985). "Localization of tubulin binding site for tau protein". Eur. J. Biochem., **153**(3) 595-600

Serrano, L., J. De La Torre, R.B. Maccioni, J. Avila (1984). “Biochemistry Involvement of the carboxyl-terminal domain of tubulin in the regulation of its assembly.” Proc. Natl. Acad. Sci., **81**: 5989-5993.

Sharma, S., C. Lagisetti, B. Poliks, R. M. Coates, D. G. Kingston and S. Bane (2013). "Dissecting paclitaxel-microtubule association: quantitative assessment of the 2'-OH group." Biochemistry, **52**(13): 2328-2336.

Sindelar, C.V., K. H. Downing (2007). “The beginning of kinesin's force-generating cycle visualized at 9-Å resolution.” J. Cell Biol., **177**(3): **377-385.**

Snyder, J. P., J. H. Nettles, B. Cornett, K. H. Downing and E. Nogales (2001). "The binding conformation of Taxol in beta-tubulin: a model based on electron crystallographic density." Proc. Natl. Acad. Sci., **98**(9): 5312-5316.

Tanaka, J. I., Higa T. (1996). "Zampanolide, a new cytotoxic macrolide from a marine sponge." Tetrahedron Letters, **37**(31): 5535-5538.

Tang, G., L. Peng, P. Baldwin, D.S. Mann, W. Jiang, I. Rees, S. J. Ludtke (2007). “EMAN2: an extensible image processing suite for electron microscopy.” J. Struct. Biol., **157**(1): 38-46.

Tennstaedt, A., S. Popsel, L. Truebestein, P. Hauske, A. Brockmann, N. Schmidt, B. Sacca, C.M. Neimeyer, R. Brandt, H. Kseizak-Reding, A. L. Tirnicerius, R. Egensperger, A. Baldi, L. Dehmelt, M. Kaiser, R. Huber, T. Clausen, M. Ehrmann (2012). "Human high temperature requirement serine protease A1 (HTRA1) degrades tau protein aggregates." J. Biol. Chem., **287**(25): 20931-41

Ter Haar, E., R. J. Kowalski, E. Hamel, C. M. Lin, R. E. Longley, S. P. Gunasekera, H. S. Rosenkranz and B. W. Day (1996). "Discodermolide, a cytotoxic marine agent that stabilizes microtubules more potently than Taxol." Biochemistry **35**(1): 243-250.

Tilney, L. G., Bryan, J., Bush, D. J., Fujiwara, K., Mooseker, M. S., Murphy, D. B., Snyder, D. H. (1973). "Microtubules: evidence for 13 protofilaments." J. Cell Biol., **59**, 267-275.

Tompa, P. (2012). "Intrinsically disordered proteins: a 10-year recap." Trends Biochem. Sci., **37**(12): 509–516.

Trinczek, B., Ebneth, A., Mandelkow, E. M., Mandelkow, E. (1999). "Tau regulates the attachment/detachment but not the speed of motors in microtubule-dependent transport of single vesicles and organelles." J. Cell Sci. **112**: 2355–67.

Van de Mark, D., D. Kong, J. Loncarek, T. Stearns. (2015). "MDM1 is a microtubule-binding protein that negatively regulates centriole duplication." Cytoskeleton, **26**(21): 3788-3802.

Venier, P., A. C. Maggs, M. F. Carlier and D. Pantaloni (1994). "Analysis of microtubule rigidity using hydrodynamic flow and thermal fluctuations." J. Biol. Chem., **269**(18): 13353-13360.

Voter, W. A., Erickson, H. P. (1982). "Electron micrscopy of MAP 2 (microtubule-associated protein 2)." J. Ultrastruct. Res., **80**: 374-82.

Wade, R. H., D. Chretien, D. Job (1990). "Characterization of microtubule protofilament numbers. How does the surface lattice accommodate?" J. Mol. Biol., **212**(4): 775-786.

Wang, Y., S. Yin, K. Blade, G. Cooper, D. R. Menick and F. Cabral (2006). "Mutations at leucine 215 of beta-tubulin affect paclitaxel sensitivity by two distinct mechanisms." Biochemistry **45**(1): 185-194.

Wani, M. C., H. L. Taylor, M. E. Wall, P. Coggon, A. T. McPhail (1971). "Plant antitumor agents. VI. The isolation and structure of Taxol, a novel antileukemic and antitumor agent from Taxus brevifolia." J. Am. Chem Soc., **93**(9): 2325-2327.

Weingarten, M., Lockwood, A., Hwo, S., and Kirschner, M. (1975). "A protein factor essential for microtubule assembly." Proc. Natl. Acad. Sci. **72**: 1858-62.

West, L. M., P. T. Northcote and C. N. Battershill (2000). "Peloruside A: a potent cytotoxic macrolide isolated from the new zealand marine sponge Mycale sp." J Org Chem **65**(2): 445-449.

Wilmes, A., K. Bargh, C. Kelly, P. T. Northcote and J. H. Miller (2007). "Peloruside A synergizes with other microtubule stabilizing agents in cultured cancer cell lines." Mol. Pharm., **4**(2): 269-280.

Write P. E., H. J. Dyson (2009). “Linking folding and binding.” Curr. Opin. Struct. Biol., **12**: 31-38.

Xiao, H., P. Verdier-Pinard, N. Fernandez-Fuentes, B. Burd, R. Angeletti, A. Fiser, S. B. Yin, S., F. Cabral and S. Veeraraghavan (2007). "Amino acid substitutions at proline 220 of beta-tubulin confer resistance to paclitaxel and colcemid." Mol. Cancer Ther., **6**(10): 2798-2806.

Zhang, R. and E. Nogales (2015). "A new protocol to accurately determine microtubule lattice seam location." J. Struct. Biol., **192**(2): 245-254.

Zhang, R., G. M. Alushin, A. Brown and E. Nogales (2015). "Mechanistic Origin of Microtubule Dynamic Instability and Its Modulation by EB Proteins." Cell, **162**(4): 849-85